

## The CGM with local universe FRBs: evidence of strong AGN feedback in a massive elliptical galaxy

SAMUEL MCCARTY ,<sup>1</sup> LIAM CONNOR ,<sup>1</sup> AND RALF M. KONIETZKA <sup>1</sup><sup>1</sup> *Center for Astrophysics | Harvard & Smithsonian*

## ABSTRACT

Modern cosmology and galaxy formation rely on an understanding of how cosmic baryons are distributed, a significant portion of which exist in the diffuse gas confined to halos. Fast Radio Bursts (FRBs) are a promising probe of the Universe’s ionized gas. At low redshift, the contribution to the dispersion measure (DM) from the intergalactic medium (IGM) and intervening halos is subdominant, allowing us to study the circumgalactic media (CGM) of the host galaxies. We select a sample of five local universe FRBs whose host interstellar medium (ISM) DM is negligible and use these to constrain the mass of the CGM in each halo. We find that one of our sources, the only massive elliptical host galaxy, has been evacuated of its baryons ( $M_{\text{gas}} = 0.02^{+0.02}_{-0.02} M_{\text{h}}$ , corresponding to  $\sim 10\%$  of the cosmological average  $\frac{\Omega_b}{\Omega_m}$ ). This galaxy shows evidence of a past episode of AGN activity, consistent with the picture of strong AGN feedback in galaxy group-scale halos. The other sources are consistent with existing multiwavelength data and tentatively support more baryon retention in  $L_*$  galaxies compared to group-scale halos. We show that FRBs can measure the halo gas fraction  $f_{\text{gas}}$  in halos of mass  $M_{\text{h}} \sim 10^{11-13} M_{\odot}$ , and up to  $\sim 10^{14} M_{\odot}$  if galaxy cluster hosts are included, which is a larger range than other gas probes can access. Finally, we demonstrate that a large sample of local universe FRBs, such as those expected from upcoming all-sky radio telescopes, will enable precision measurements of halo gas, which is crucial for understanding the effects of feedback.

## 1. INTRODUCTION

The nature of the gas gravitationally bound to dark matter halos is a key limiting factor in our understanding of galaxy formation and cosmology. For galaxies, this circumgalactic medium (CGM) acts as an interface with the galaxy’s cosmological environment. It plays a key role in the baryon cycle, which controls the growth of the galaxy through accretion from the intergalactic medium (IGM), feedback processes, and recycling (J. Tumlinson et al. 2017). For cosmology, the suppression of the matter power spectrum due to baryonic effects on small scales is a leading source of uncertainty in the upcoming Stage IV weak lensing surveys by the *Euclid* satellite (Y. Mellier et al. 2025), the Vera C. Rubin Observatory (Z. Ivezic et al. 2019), and the *Nancy Roman Space Telescope* (D. Spergel et al. 2013), thus complicating our understanding of dark matter and dark energy (e.g. E. Semboloni et al. (2011)). Further, the relative amount of baryons in different components of the diffuse gas (the CGM, IGM, intragroup medium, intracluster medium) has been debated for decades – often

referred to as “missing baryons problem” (R. Cen & J. P. Ostriker 1999).

While traditional probes of halo gas have made significant progress this decade, they have several drawbacks. It is difficult to detect low to intermediate-mass halos in X-ray or the Sunyaev-Zeldovich (SZ) effect (R. A. Sunyaev & Y. B. Zeldovich 1972). The thermal Sunyaev-Zeldovich effect (tSZ) and X-rays further rely on assumptions about gas temperature and metallicity, respectively. The kinetic Sunyaev-Zeldovich (kSZ) signal is intrinsically faint, such that it has only been measured for galaxy group-scale and larger halos (e.g. E. Schaan et al. (2021), B. R. Guachalla et al. (2025)). Quasar absorption spectroscopy relies on assumptions about ionization state and structure of the gas (J. Tumlinson et al. 2017).

On the other hand, Fast Radio Bursts (FRBs) have emerged as a promising new method of studying the gas in and around halos. FRBs are millisecond radio transients whose signals are dispersed as they travel through cosmic plasma (D. R. Lorimer et al. 2007; E. Petroff et al. 2019; J. M. Cordes & S. Chatterjee 2019). The dispersion measure (DM) of FRBs is a clean probe of electron column density along the line of sight (E. Petroff et al. 2019):

$$\text{DM}(z) = \int_0^z \frac{n_e(z')c}{(1+z')^2 H(z')} dz', \quad (1)$$

where  $n_e$  is the electron density and  $H(z)$  is the Hubble parameter.

Significant progress has been made towards using FRBs as astrophysical and cosmological tools. One approach studies the distribution of observed DM as a function of redshift to constrain the IGM and feedback (M. McQuinn 2013; J.-P. Macquart et al. 2020; R. Reischke & S. Hagstotz 2025; L. Connor et al. 2025; K. Sharma et al. 2025b). Others correlate the FRB signal with various observables (R. Reischke et al. 2024; M. Hussaini et al. 2025; H. Wang et al. 2025; C. Leung et al. 2025a; K. Sharma et al. 2025a; R. Takahashi et al. 2025; C. Leung et al. 2025b). However, much work remains to be done towards studying the gas in halos with FRBs. One promising approach is to use FRBs intersecting intervening halos along the line of sight (L. Connor & V. Ravi 2022; X. Wu & M. McQuinn 2023; I. S. Khrykin et al. 2024; M. Hussaini et al. 2025), although this is limited by the current FRB sample size. There have been a few investigations of groups/clusters (L. Connor et al. 2023; K.-G. Lee et al. 2023; A. E. Lanman et al. 2025) and targeted studies of FRBs intersecting M31 (L. Connor et al. 2020; R. Anna-Thomas et al. 2025). C. Leung et al. (2025b) investigated the relationship between host galaxy DM and stellar mass for a sample of local universe FRBs. They found an anti-correlation, which aligns more closely with simulations that have stronger feedback implementations, constraining feedback in  $M_h \sim 10^{11-13} M_\odot$  halos.

The Milky Way (MW) CGM itself is an obvious target, and recent works have placed upper limits on its integrated DM (F. Kirsten et al. 2022; A. M. Cook et al. 2023; V. Ravi et al. 2025). However, these studies were dominated by individual low-DM FRBs. Utilizing larger samples of FRBs, such as the recent work by J. Hoffmann et al. (2026), will enable a more comprehensive characterization of the MW CGM, and may enable detection of anisotropies (J. X. Prochaska & Y. Zheng 2019; Y. Liu et al. 2026).

In addition to the MW, FRBs offer a critical opportunity to study the CGM in  $10^{11-13} M_\odot$  halos which has so far been largely untapped. In this work, we propose to use local universe FRBs for this purpose. Below  $z \lesssim 0.2$ , the DM budget is no longer dominated by the cosmic web, allowing the contribution from the CGM of the host to be more easily isolated.

Because it is not in general possible to disentangle the DM from the host interstellar medium (ISM) and host CGM, we select a sample of FRBs for which there

is reason to believe that ISM DM is small (Section 2). We analyze this sample in Section 3 to determine the gas content of the host halos. In Section 4 we provide a discussion of our results and future prospects for this method in light of upcoming all-sky monitors. Throughout this work we assume the best-fit Planck 2018+BAO cosmology ( Planck Collaboration et al. 2020).

## 2. FRB SAMPLE AND DM ACCOUNTING

The observed DM of an FRB can be divided into several parts:

$$\text{DM}_{\text{obs}} = \text{DM}_{\text{MW,ISM}} + \text{DM}_{\text{MW,CGM}} + \text{DM}_{\text{cosmic}} + \frac{\text{DM}_{\text{host}}}{1+z} \quad (2)$$

$$\text{DM}_{\text{host}} = \text{DM}_{\text{host,ISM}} + \text{DM}_{\text{host,CGM}}. \quad (3)$$

$\text{DM}_{\text{MW,ISM}}$  and  $\text{DM}_{\text{MW,CGM}}$  are the contributions from the gas in the MW's ISM and CGM, respectively, and  $\text{DM}_{\text{host,x}}$  refers to the same for the FRB host galaxy.  $\text{DM}_{\text{cosmic}}$  is the contribution from the IGM and intervening halos along the line of sight. Note that some authors distinguish further a DM component from circumburst material in the local environment of the FRB, we group this into  $\text{DM}_{\text{host,ISM}}$ .

We wish to isolate the  $\text{DM}_{\text{host,CGM}}$  term. Under the assumption that different components of the DM are independent, which is not in general true but a good approximation (see e.g. (R. M. Konietzka et al. 2025) for the correlation between  $\text{DM}_{\text{host}}$  and  $\text{DM}_{\text{cosmic}}$ ), the probability density function (PDF) can be written:

$$p\left(\frac{\text{DM}_{\text{host,CGM}}}{1+z}\right) = p(\text{DM}_{\text{obs}}) * p(-\text{DM}_{\text{MW,ISM}}) * p(-\text{DM}_{\text{MW,CGM}}) * p(-\text{DM}_{\text{cosmic}}) * p\left(\frac{-\text{DM}_{\text{host,ISM}}}{1+z}\right). \quad (4)$$

### 2.1. Cosmic DM

In previous studies the contribution of the cosmic web towards the total DM,  $p(\text{DM}_{\text{cosmic}}|z)$ , has been modeled using the parameterization presented in J.-P. Macquart et al. (2020). However, recent work suggests that this prescription of  $p(\text{DM}_{\text{cosmic}}|z)$  does not fully capture the higher-order moments of the distribution (R. M. Konietzka et al. 2025; K. Sharma et al. 2025b). Therefore, in this work, we use the best-fit functional form from R. M. Konietzka et al. (2025) for  $p(\text{DM}_{\text{cosmic}}|z)$ , which is described by a modified-normal density function with a power-law tail at the high DM end:

$$p(\text{DM}_{\text{cosmic}}|z) = c \exp\left(-\frac{\mu^2 \left(\left(\frac{\mu}{x}\right)^\alpha - 1\right)^2}{2\sigma^2 \alpha^2}\right) \left(\frac{\mu}{x}\right)^\beta \quad (5)$$

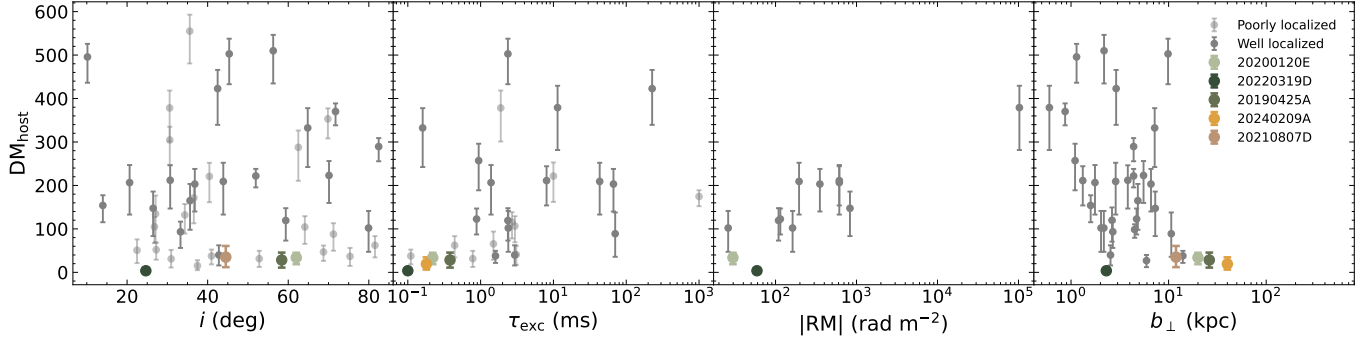


**Figure 1.**  $DM_{\text{host}}$  for all localized FRBs with  $z < 0.2$  at the time of writing plotted against potential indicators of  $DM_{\text{host,ISM}}$ : host galaxy inclination  $i$ , scattering timescale  $\tau_{\text{exc}}$ , rotation measure RM, and impact parameter  $b_{\perp}$ . The colored points are the five FRBs selected for our analysis. Light grey points are the poorly localized ( $\sim$ arcmin) FRBs.

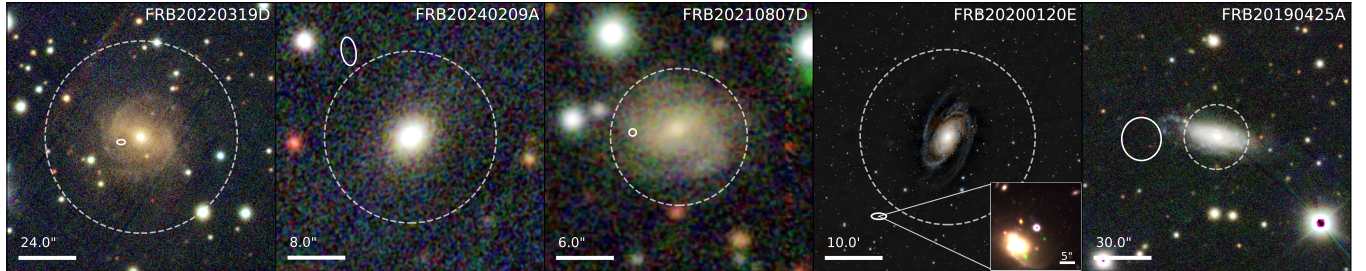


**Figure 2.** Pan-STARRS1 (K. C. Chambers et al. 2019) gri color images of the FRB host galaxies in our sample. The FRB localization regions are shown as solid white ellipses. The dashed white circles are  $0.1R_{500c}$  for each galaxy's halo. For FRB20200120E, the inset shows the VLBI localization to a globular cluster in M81 presented by F. Kirsten et al. (2022).

where the normalization constant  $c$  can be obtained via

$$c^{-1} = \frac{\mu}{\alpha} e^{-\frac{\eta^2}{2}} \left( \frac{\alpha \sigma}{\mu} \right)^{\delta} \Gamma(\delta) D_{-\delta} \left( -\sqrt{2} \eta \right), \quad (6)$$

where  $\delta = \frac{\beta-1}{\alpha}$ ,  $\eta^2 = \frac{\mu^2}{2\sigma^2 \alpha^2}$ ,  $\Gamma(\cdot)$  is the gamma function and  $D(\cdot)$  the parabolic cylinder function. As in R. M. Konietzka et al. (2025), we use shape parameters  $\alpha \approx 1$  and  $\beta \approx 3.3$ . The remaining two parameters  $\mu$  and  $\sigma$  are tuned using simulated DM (R. M. Konietzka et al. 2025) drawn from the IllustrisTNG simulation (D. Nelson et al. 2021). To this end, we make use of the continuous DM catalog<sup>2</sup> provided in R. M. Konietzka et al. (2025) that traces rays through the IllustrisTNG simulation while reconstructing all traversed line segments within the underlying Voronoi mesh. Although this relation is fit to the IllustrisTNG simulation, we do not expect this to bias our results at the low redshifts considered in this work, as the probability of intersecting a foreground halo as well as the total expected IGM contribution for our local Universe sources is low.

## 2.2. Milky Way DM

At low redshift it is important to consider the impact of our choice of model for  $p(DM_{\text{MW,ISM}})$ , which could significantly bias our results. Popular choices for  $p(DM_{\text{MW,ISM}})$  are the NE2001 (J. M. Cordes & T. J. W. Lazio 2003; S. K. Ocker & J. M. Cordes 2024) and YMW16 J. M. Yao et al. (2017) models, which were fit to pulsar DM data. However, as seen in V. Ravi et al. (2025), these models can overestimate  $DM_{\text{MW,ISM}}$ , especially at low galactic latitudes. Because we expect  $DM_{\text{host,CGM}}$  to be  $\mathcal{O}(10 - 100)$  pc/cm<sup>3</sup>, we need to be more conservative. For this reason we follow V. Ravi et al. (2025) and consider independent estimates of  $DM_{\text{MW,ISM}}$ . First, we estimate  $DM_{\text{MW,ISM}}$  for a given FRB sightline using the scaling between the neutral hydrogen column  $N_{\text{H}}$  and DM found by C. He et al. (2013). The column densities are retrieved from the HI4PI survey (HI4PI Collaboration: et al. 2016). The associated uncertainty comes from the scatter in the relationship. Next, we use the H $\alpha$  emission measure (EM) to estimate  $DM_{\text{MW,ISM}}$ . The H $\alpha$  flux data is obtained from the Wisconsin H $\alpha$  Mapper (WHAM) (L. M. Haffner et al. 2003), and the analysis follows E. M. Berkhuijsen et al. (2006). The H $\alpha$  flux is corrected for dust reddening and

<sup>2</sup> The continuous DM catalog along with other DM maps and catalogs from R. M. Konietzka et al. (2025) can be downloaded at <https://ralfkonietzka.github.io/fast-radio-bursts/ray-tracing-catalogs/>.

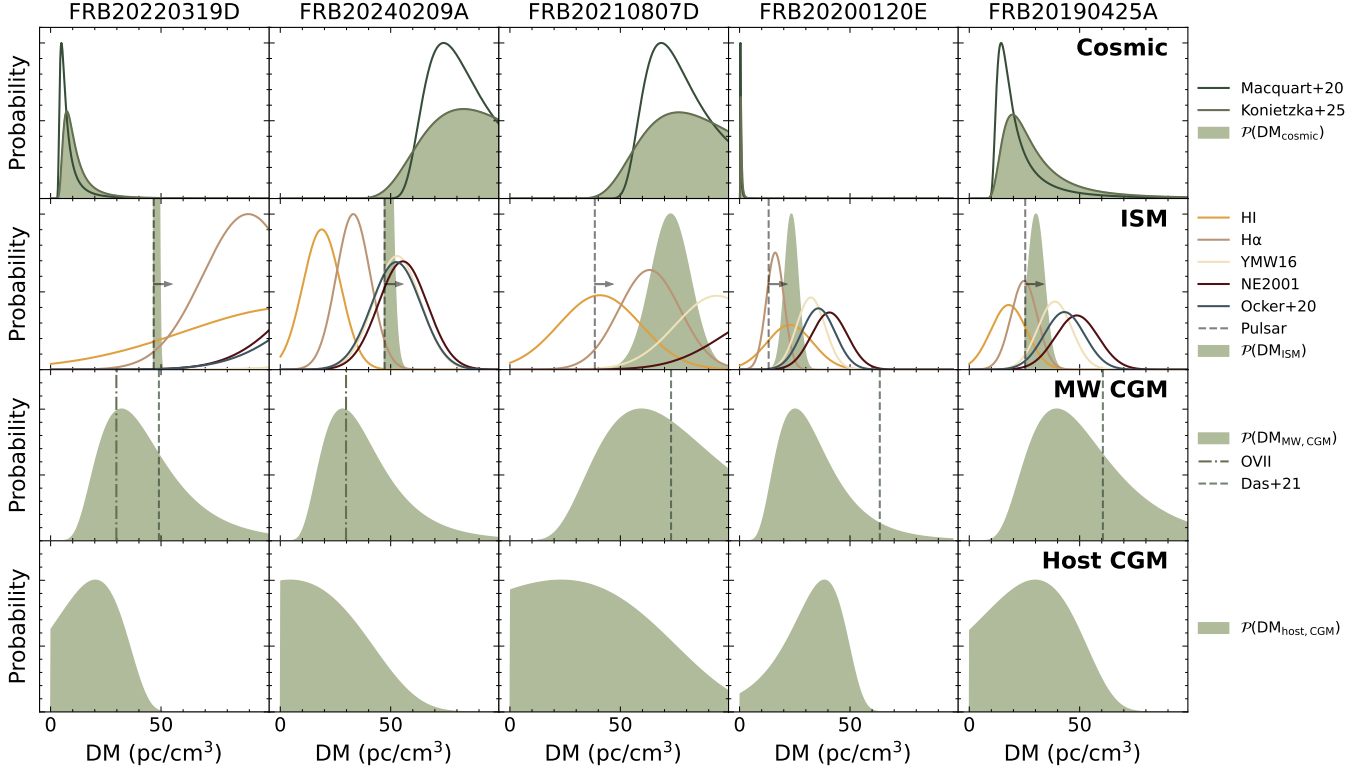


**Figure 3.** The PDFs of the different DM components using various estimates, with the shaded curves showing the adopted PDFs used in our analysis. In each plot, all curves are arbitrarily scaled by the same factor for better visualization. The top row shows  $p(\text{DM}_{\text{cosmic}})$ , which is estimated using the best fit of R. M. Konietzka et al. (2025), with the relation of J.-P. Macquart et al. (2020) plotted for reference. The middle row shows  $p(\text{DM}_{\text{MW,ISM}})$ , where the final PDF is the combination of the HI, H $\alpha$ , and YMW16 (J. M. Yao et al. 2017) estimates, truncated by the pulsar lower limit (vertical dashed line). For FRB 20220319D, the mean  $\text{DM}_{\text{MW,ISM}}$  estimate is much larger than  $\text{DM}_{\text{obs}}$ , so we set  $p(\text{DM}_{\text{MW,ISM}})$  as a delta function at the pulsar lower limit following (V. Ravi et al. 2025). We also show the NE2001 (J. M. Cordes & T. J. W. Lazio 2003; S. K. Ocker & J. M. Cordes 2024) and S. K. Ocker et al. (2020) models for comparison. The third row shows YT20 (S. Yamasaki & T. Totani 2020) estimate of  $\text{DM}_{\text{MW,CGM}}$ . We also plot an estimate of  $\text{DM}_{\text{MW,CGM}}$  using the nearest OVII absorption sightline to each FRB from T. Fang et al. (2015) and the scaling relation between  $N_{\text{OVII}}$  and DM from (S. Yamasaki & T. Totani 2020), as well as the median of sightlines within 20° from S. Das et al. (2020) (but note that the uncertainty in both of these is quite large). In the bottom panel, we plot the final  $p(\text{DM}_{\text{host}})$ , which under our assumption of negligible  $\text{DM}_{\text{host,ISM}}$  becomes  $p(\text{DM}_{\text{host,CGM}})$ .

converted to an EM with associated uncertainty assuming a mean electron temperature  $T_e = 8000$  K. Because  $\text{DM} \propto n_e l$ , where  $l$  is the distance, and  $\text{EM} \propto n_e^2 l$ , we can estimate  $\text{DM} \sim \sqrt{\text{EM}l}$ , with some assumption about the structure of the gas for which we follow V. Ravi et al. (2025). To estimate the distance through the ISM for extragalactic FRBs we assume the ISM is a disk with height 1.25 kpc (E. M. Berkhuijsen et al. (2006) find the average electron density  $\langle n_e \rangle$  is constant to a height of  $\sim 1$  kpc and then drops off with a scale length  $\sim 0.3$  kpc), and an uncertainty on this distance of 20%.

With the HI and H $\alpha$  estimates in hand, we combine these with the pulsar-based estimates, the NE2001 and YMW16 models (assuming 20% uncertainty on each), to get a final distribution  $p(\text{DM}_{\text{MW,ISM}})$ . We further identify the closest pulsar to each FRB sightline within 1 degree of galactic latitude from the ANTF pulsar cata-

logue<sup>3</sup> (R. N. Manchester et al. 2005), excluding globular cluster pulsars, and use the DM of the pulsar as a hard lower limit by truncating  $p(\text{DM}_{\text{MW,ISM}})$ . Each FRB is within 10 degrees of the nearest pulsar. In a special case for FRB 20220319D, the  $\text{DM}_{\text{MW,ISM}}$  estimate is much larger than the total  $\text{DM}_{\text{obs}}$ , so we follow V. Ravi et al. (2025) and use only the pulsar lower limit instead (a delta function for  $p(\text{DM}_{\text{MW,ISM}})$ ). By combining multiple independent estimates, we aim to mitigate the risk of systematically overestimating  $\text{DM}_{\text{MW,ISM}}$ .

To estimate  $\text{DM}_{\text{MW,CGM}}$  we use the model of S. Yamasaki & T. Totani (2020) (hereafter YT20), which is fit to X-ray EM data. In general there is a lack of independent data available to constrain this component, we

<sup>3</sup> <https://www.atnf.csiro.au/research/pulsar/psrcat>

take the YT20 model as a conservative estimate, and discuss the impact of  $\text{DM}_{\text{MW,CGM}}$  in Section 4.4. We include a lognormal scatter of 0.2 dex around the YT20 value for each FRB sightline .

### 2.3. Host DM

It remains to separate the  $\text{DM}_{\text{host,ISM}}$  and  $\text{DM}_{\text{host,CGM}}$  components. Our approach is to select a sample of FRBs for which  $\text{DM}_{\text{host,ISM}}$  is negligible. In the future, it may be possible to estimate  $\text{DM}_{\text{host,ISM}}$  independently (from resolved integral-field unit observations of  $\text{H}\alpha$  in the host galaxy for example), but it is not feasible with available data. However, several properties of the FRBs and their host galaxies are indicative of low  $\text{DM}_{\text{host,ISM}}$ , allowing us to be smart with our sample selection. In particular, we identify the host galaxy inclination  $i$ , the FRB scattering timescale  $\tau_{\text{exc}}$  (with MW contribution subtracted), the FRB rotation measure (RM), and the impact parameter of the FRB to the host galaxy  $b_{\perp}$  as promising indicators. An FRB originating from the disk of a face-on spiral galaxy will have traveled less distance through the host ISM than an edge-on spiral, so we expect  $i$  to correlate with  $\text{DM}_{\text{host,ISM}}$  (M. Bhardwaj et al. 2024). Similarly, we expect the local environment and host ISM to be the main contributors to the scattering and RM of the FRB. This is because the ISM and circumstellar material can produce density fluctuations appropriate for Faraday rotation and strong scattering; in the IGM (J. Luan & P. Goldreich 2014) and CGM this is much less likely (H. K. Vedantham & E. S. Phinney 2019). Finally, the farther away from the host galaxy the FRB originates, the less ISM gas it will encounter. Indeed, R.-N. Li et al. (2025) find a correlation between extragalactic DM and  $\text{cos}i$ ,  $\tau_{\text{exc}}$ , and  $b_{\perp}$ .

To test this hypothesis and select an FRB sample, we first start with all localized FRBs in the literature. We apply an initial cut of  $z < 0.2$ , leaving 67 FRBs. We compile stellar mass  $M_*$ ,  $i$ ,  $\tau_{\text{exc}}$ ,  $b_{\perp}$ , and RM data, borrowing heavily from Table 1 of R.-N. Li et al. (2025). In Figure 1 we have plotted  $\text{DM}_{\text{host}} = \text{DM}_{\text{host,ISM}} + \text{DM}_{\text{host,CGM}}$  of each FRB, determined by subtracting from  $\text{DM}_{\text{obs}}$  the DM component estimates described above, against each  $\text{DM}_{\text{host,ISM}}$  indicator. It is clear that  $\tau_{\text{exc}}$ , RM, and  $b_{\perp}$  are correlated with  $\text{DM}_{\text{host,ISM}}$ .  $i$  does not appear to correlate strongly by eye, which aligns with the relatively weaker correlation found by R.-N. Li et al. (2025). With this information, we select five FRBs that we deem likely to have little  $\text{DM}_{\text{host,ISM}}$  contribution for our analysis. We are following a similar prescription proposed by C. Leung et al. (2025b) but with a more aggressive cut in

inclination angle. We select only from the FRBs whose localization is sufficient to determine a reliable  $b_{\perp}$  with respect to the host galaxy. The FRBs and our reasoning for selecting them are described below, with notable properties summarized in Table 1. Figure 2 shows the FRB’s host galaxies and localizations. Figure 3 shows in detail the estimates of the DM components as described above for each FRB.

*FRB 20220319D* – Reported in C. J. Law et al. (2024) and analyzed in V. Ravi et al. (2025), FRB 20220319D has one of the lowest  $\text{DM}_{\text{obs}}$  of any FRB. This was exploited in V. Ravi et al. (2025) to place a tight constraint on the CGM of the MW. This FRB has a very small  $\tau_{\text{exc}}$ , low RM, and the host galaxy is a nearly face-on spiral, making it an excellent candidate for our sample.

*FRB 20240209A* – This is the only known FRB originating from an isolated massive elliptical galaxy (V. Shah et al. 2025; T. Eftekhari et al. 2025).  $b_{\perp}$  is 5 times the effective radius of the galaxy, meaning that the FRB likely comes from a globular cluster and has almost no  $\text{DM}_{\text{host,ISM}}$ .  $\tau_{\text{exc}}$  is also very small, aligning with this idea. FRB 20240209A is also an attractive target for our study because we expect AGN feedback to alter the CGM in halos of this mass (I. G. McCarthy et al. 2010; K. Schawinski et al. 2007), which is discussed in Section 4.2.

*FRB 20210807D* – This FRB has a large  $b_{\perp}$  and low inclination (A. C. Gordon et al. 2023; R. M. Shannon et al. 2025). We include it in our sample with the caveat that it appears to have a non-negligible scattering (Figure B1 in R. M. Shannon et al. (2025)). This means that a measurement of its CGM is more likely an upper limit (Section 3).

*FRB 20200120E* – A very nearby FRB originating from a globular cluster in M81 (M. Bhardwaj et al. 2021; F. Kirsten et al. 2022). This is the lowest  $\text{DM}_{\text{obs}}$  FRB at the time of writing, and an excellent candidate for our sample because it will have encountered little host ISM gas. Accordingly, it has a low RM and  $\tau_{\text{exc}}$ .

*FRB 20190425A* – This CHIME FRB’s host galaxy is sufficiently nearby such that the  $b_{\perp}$  is not terribly uncertain even without arcsec localization (M. Bhardwaj et al. 2023). It is included in our sample because of the large  $b_{\perp}$  and low  $\tau_{\text{exc}}$ .

We note that our measurements of  $\text{DM}_{\text{host,CGM}}$  are actually conservative upper limits because of our DM accounting choices and because it is always possible to have contributions to the DM that are not included in the analysis, which we explain in the following.

Our  $\text{DM}_{\text{MW,ISM}}$  estimates are lower than the NE2001 or YMW16 models, which are widely adopted for FRB science, and recent work indicates that  $\text{DM}_{\text{MW,CGM}}$

FRB	20220319D	20240209A	20210807D	20200120E	20190425A
RA	32.17792	289.88750	299.22143	149.47783	255.67500
DEC	71.03526	86.06444	-0.76236	68.81889	21.57639
DM <sub>obs</sub>	110.95	176.52	251.30	87.82	128.20
$z$	0.0112	0.1384	0.1293	0.0008	0.0312
$\log_{10} M_*/M_\odot$	9.93	11.34	10.94	10.86	10.26
$\log_{10} M_{\text{h,vir}}/M_\odot$	11.6	13.2	12.4	12.3	11.8
$b_\perp$ (kpc)	2.3	40	11.91	20	26.13
References	1, 2	3, 4	5, 6	7, 8	9

**Table 1.** FRB and host galaxy properties.  $M_{\text{h,vir}}$  is inferred from the stellar mass-halo mass relation with an associated uncertainty of 0.2 dex (P. Behroozi et al. 2019). 1. C. J. Law et al. (2024) 2. V. Ravi et al. (2025) 3. V. Shah et al. (2025) 4. T. Ettekhari et al. (2025) 5. R. M. Shannon et al. (2025) 6. A. C. Gordon et al. (2023) 7. M. Bhardwaj et al. (2021) 8. F. Kirsten et al. (2022) 9. M. Bhardwaj et al. (2023)

may exceed the predictions of the YT20 model (Section 4.4). Other bodies of gas that were not accounted for, such as a Local Group medium, M31, or the Magellenic clouds, could contribute tens of pc cm<sup>-3</sup> to the observed DM (J. X. Prochaska & Y. Zheng 2019), tightening the constraints. Further, we have selected a sample of FRBs whose DM<sub>host,ISM</sub> is small, but because DM<sub>host</sub> is  $\mathcal{O}(10 - 100)$  pc cm<sup>-3</sup> it may still be a significant contribution. Finally, M81 actually resides in a galaxy group, and FRB 20200120E passes within 60 kpc of M82 (halo mass roughly half of M81 (M. Bhardwaj et al. 2021)). If we included M82 in our analysis, the measured DM<sub>host,CGM</sub> of M81 would decrease accordingly. Other FRBs in our sample and future samples may have companion or satellite galaxies as well.

Finally, in Section 3.2 we include a sixth FRB in our analysis with a galaxy cluster host, to demonstrate the range of halo masses accessible with FRBs. This is the local universe cluster FRB 20220509G from L. Connor et al. (2023). In this case the interpretation is different than for our main sample because we are now probing the intra-cluster medium (ICM). For this FRB, we perform the same analysis as for our main sample, but we further subtract a DM<sub>host</sub> component which represents the gas associated with the subhalo/galaxy from which the FRB originates. For the DM<sub>host</sub> PDF we use the best-fit lognormal from L. Connor et al. (2025). This FRB is included for demonstration but does not drive the results.

### 3. ANALYSIS

Now that we have isolated DM<sub>CGM</sub> for our sample, we can use this to study the gas in these halos. DM<sub>CGM</sub> is an integral of the electron density through the halo and so depends on both the radial profile, through  $b_\perp$ , and the overall normalization (the total amount of gas in the halo). As a function of halo mass, both of these pieces are of scientific interest and encode information about

feedback processes. Throughout this work, we use the stellar mass-halo mass relation from (P. Behroozi et al. 2019) to convert the host galaxy stellar mass measurements.

#### 3.1. Comparison to simulations

First, we compare our measurements to the halos seen in simulations. We use the IllustrisTNG (TNG) (D. Nelson et al. 2021; A. Pillepich et al. 2017; V. Springel et al. 2017; D. Nelson et al. 2017; J. P. Naiman et al. 2018; F. Marinacci et al. 2018) and SIMBA (R. Davé et al. 2019) simulations. Specifically, for TNG we use the TNG100-2 run, having a minimum particle gas mass of  $1.1 \times 10^7 M_\odot$ . For SIMBA, we use the m100n1024 run with the fill s50 physics, and a gas mass resolution of  $1.82 \times 10^7 M_\odot$ . We choose TNG100-2 over TNG100-1 because the resolution is closer to SIMBA, but verify that moving to TNG100-1 does not change the results significantly. These two simulations are a good point of comparison because they will have different halo gas contents due to different AGN feedback implementations, especially at masses  $\gtrsim 10^{12} M_\odot$  (B. D. Oppenheimer et al. 2021). We expect SIMBA to have gas-poor halos relative to TNG because of the stronger AGN feedback. SIMBA also provides versions of their simulation run with AGN feedback turned off (s50noagn), which we include in our analysis with the same box size. Although both the TNG and SIMBA simulations assume the Planck 2016 cosmology, we do not expect our results to be sensitive to small changes in the cosmology (P. A. R. Ade et al. 2016). For each FRB and each simulation, we randomly select 100 halos uniformly in log space within 0.2dex of  $M_{\text{h,200c}}$  of the FRB host galaxy (the uncertainty in the (P. Behroozi et al. 2019) stellar mass-halo mass relation). We use the `yt` package to grid the simulation data uniformly in a sphere of radius  $R_{200c}$  around the center of the halo. We integrate the electron density along the positive and negative directions of each

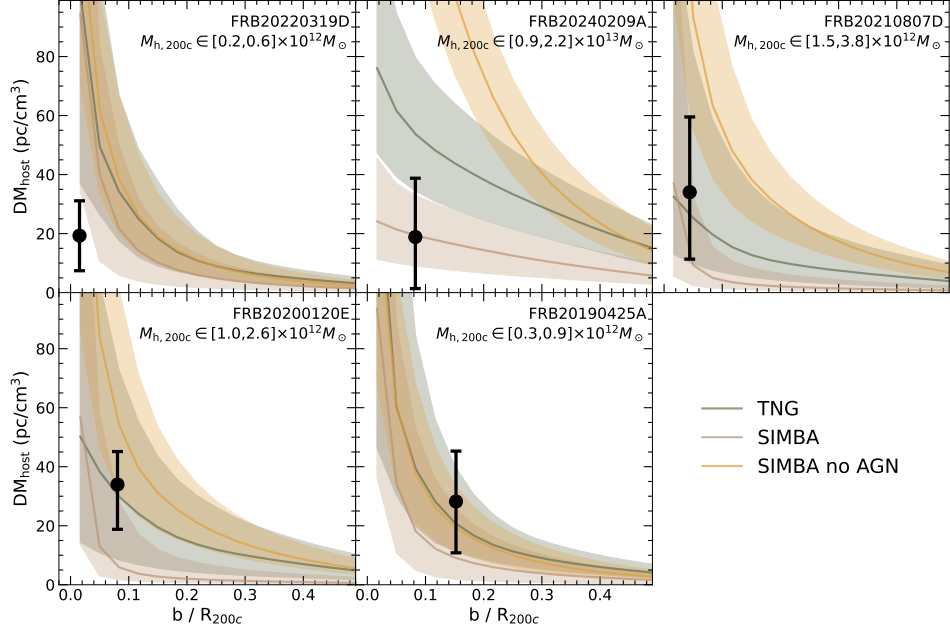


**Figure 4.**  $\text{DM}_{\text{host}}$  vs. normalized impact parameter through the halo  $b_{\perp}/R_{200c}$ . Each panel shows the measurement from an FRB in our sample (in black) and randomly selected halos from simulations within 0.2 dex of the FRB host  $M_{h,200c}$ . We show three simulations: IllustrisTNG (TNG50) (D. Nelson et al. 2021), SIMBA (R. Davé et al. 2019), and SIMBA with AGN feedback turned off. Solid lines are the median values, and shaded regions are the 16th and 84th percentile intervals, capturing both sightline-to-sightline variance within each halo and halo-to-halo variance.

axis to get the DM, stopping at the midplane of the halo. Therefore, we have many sightlines for a given normalized  $b_{\perp}/R_{200c}$ , capturing both the sightline-to-sightline variance within a halo and the variance between the 100 halos.

We are assuming that the FRB is located exactly halfway through the halo along the line of sight. This is a good approximation for FRBs 20220319D, 20210807D, 20200120E, and 20190425A, where the FRB is very likely coming from the disk. For FRB 20240209A the situation is less clear. At an impact parameter of 40 kpc, it is likely that FRB 20240209A originates from a globular cluster or satellite galaxy in its host. To quantify the likelihood that FRB 20240209A lies a given depth into the host halo, we use the distribution of globular clusters measured around M87 (W. E. Harris 2009). M87 is a large elliptical galaxy of comparable mass to the host of FRB 20240209A. The M87 system has thousands of detectable globular clusters due to its proximity. W. E. Harris (2009) find that the log of the globular cluster surface density in M87 decreases radially as  $(r/R_{\text{eff}})^{1/4}$ , where  $R_{\text{eff}}$  is the effective radius of the galaxy. We make the assumption that this relation holds for the host of FRB 20240209A, and use it to determine that FRB 20240209A lies within  $\sim \pm 40$  kpc of the midplane of the halo at  $1\sigma$  uncertainty. Assuming reasonable galaxy gas profiles (see the next section), this shift would change the measured DM by up to  $\sim 25\%$ . We include this

as additional uncertainty on the measured DM of FRB 20240209A.

The results are plotted in Figure 4. Note that below roughly  $0.1R_{200c}$  there will start to be contributions to the DM from the ISM in the simulated halos, but we have not subtracted any  $\text{DM}_{\text{host,ISM}}$  component from the FRB data, so they are still comparable.

Examining the case of FRB 20240209A, the data appear to favor the SIMBA simulation, but are also consistent with TNG within the uncertainty. On the other hand, the measurement definitively rules out the SIMBA no AGN feedback scenario. Without AGN feedback, halos of this mass ( $\sim 10^{13} M_{\odot}$ ) may retain too many of their baryons. Better agreement with SIMBA may also indicate that a stronger AGN feedback scenario is required than that implemented in TNG, although more data is needed to confirm this.

We note that we have not yet made any assumptions about the host of FRB 20240209A, as we do in the following section (for example, spherical symmetry). Furthermore, we note that in order to bring our data point of FRB 20240209A in agreement with the no feedback scenario, or a weaker than TNG scenario, we would require either: 1) we have significantly overestimated other DM components of FRB 20240209A. For example,  $\text{DM}_{\text{MW,ISM}}$  would need to be at least a factor of 2 smaller on this sightline to bring the data above the median of the TNG curve, which is unlikely by the nearby

pulsar lower limit. 2) The host halo of FRB 20240209A is a significant outlier in terms of gas content. This is unlikely considering we have analyzed a representative population of 100 halos in each simulation. 3) FRB 20240209A is far in the foreground of the halo or not associated with the halo at all. The foreground of the halo scenario is unlikely as we discussed in the last paragraph, and the possibility that FRB 20240209A is not associated with the putative host galaxy is discussed in Section 4.3.

The other four FRBs in the sample have less constraining power, but overall agree with simulations. FRB 20220319D lies below all of the simulations, but it is difficult to compare due to contamination from the ISM at such a small impact parameter. For example, FRB 20220319D may be in the foreground of its disk, leading the simulations to pick up relatively more  $\text{DM}_{\text{host,ISM}}$ . FRBs 20210807D, 20200120E, and 20190425A seem to align more closely with the TNG simulation over the SIMBA simulation, but the uncertainty is large enough to accommodate both. These points are also higher overall than FRB 20240209A despite being at lower mass, which tentatively supports the idea that halos at  $M_h \sim 10^{12} M_\odot$  may retain a larger fraction of their baryons than more massive halos. A larger sample of local universe FRBs will provide a more stringent test of simulations and may be able to distinguish between the TNG and SIMBA simulations.

### 3.2. The halo gas fraction

To translate the DM of a single FRB sightline through a halo into a constraint on the gas mass requires assumptions about the distribution of the gas. With a large sample of FRBs at various  $b_\perp$  it would be possible to simultaneously fit the gas mass and the radial profile (Section 4.5), but that is not possible here. We perform our analysis with various profiles proposed in the literature, and use the spread in predictions between these profiles as an approximate uncertainty. In all cases, we assume a spherically symmetric profile. We continue our assumption that the FRB originates from halfway through the halo, except in the case of FRB 20240209A where we have added additional uncertainty as in the last section. Finally, we neglect the uncertainty in  $b_\perp$  due to the localization of the FRBs, as only FRB 20190425A's localization uncertainty is large enough to have an impact on the analysis (and even then it would be small).

We largely follow [J. X. Prochaska & Y. Zheng \(2019\)](#) and [L. C. Keating & U.-L. Pen \(2020\)](#). Given a radial density profile  $\rho(r)$ , normalized to the total halo mass  $M_{\text{h,vir}}$ , and impact parameter  $b_\perp$ , the observed DM is then

$$\text{DM}_{\text{host}} = \int_0^{\sqrt{r_{\text{max}}^2 - b_\perp^2}} \rho(r) f_{\text{gas}} \frac{\Omega_b}{\Omega_m} \frac{\mu_e}{m_p \mu_H} ds \quad (7)$$

where  $s$  is the path length through the halo, and  $r = \sqrt{s^2 + b_\perp^2}$ . We take  $r_{\text{max}}$  to be the halo virial radius  $R_{\text{vir}}$ , and  $\mu_e = 1.167$ ,  $\mu_H = 1.33$  for an ionized mixture of hydrogen and helium.  $f_{\text{gas}} = M_{\text{gas}} \Omega_m / M_{\text{h}} \Omega_b$  is the halo gas fraction relative to the cosmological average. Choosing  $r_{\text{max}} = R_{\text{vir}}$  means we are measuring  $f_{\text{gas,vir}} = M_{\text{gas,vir}} \Omega_m / M_{\text{h,vir}} \Omega_b$ . For our assumed cosmology,  $\Omega_b / \Omega_m = 0.1575$ .

The simplest assumption is that the halo gas follows the dark matter, well-modeled by the NFW profile ([J. F. Navarro et al. 1997](#)):

$$\rho(r) \propto \frac{1}{y(1+y)^2} \quad (8)$$

where  $y = r/r_s$ , with the scale radius  $r_s = R_{\text{vir}}/C$ , and  $C$  the concentration parameter. For all dark matter halo calculations we use the COLOSSUS package ([B. Diemer 2018](#)). We use the diemer19 model in COLOSSUS for the  $M_{\text{h}} - C$  relation so that the NFW is a single-parameter profile ([B. Diemer & M. Joyce 2019](#)).

The plain NFW profile is not a good representation of the gas in halos because we expect various baryonic effects to alter the distribution. [A. H. Maller & J. S. Bullock \(2004\)](#) proposes an alternative profile taking into account gas fragmentation:

$$\rho(r) \propto \left[ 1 + \frac{3.7}{y} \ln(1+y) - \frac{3.7}{C_c} \ln(1+C_c) \right]^{3/2} \quad (9)$$

where  $C_c = r_c/r_s$  and  $r_c$  is a cooling radius. We follow [J. X. Prochaska & Y. Zheng \(2019\)](#) and assume constant  $r_c = 147$  kpc, which is a decent approximation given that it is a weak function of halo properties and significantly larger than the impact parameters explored here, such that it shouldn't affect the results significantly.

An alternative correction to the NFW, the modified NFW (mNFW), is presented by [W. G. Mathews & J. X. Prochaska \(2017\)](#) and generalized by [J. X. Prochaska & Y. Zheng \(2019\)](#) as:

$$\rho(r) \propto \frac{1}{y^{1-\alpha} (y_0 + y)^{2+\alpha}} \quad (10)$$

where  $y_0 = \alpha = 2$  is typically chosen. Thus the inner slope of the CGM is actually rising with radius.

[G. M. Voit \(2019\)](#) create a pNFW profile, which we implement from the provided tables. The assumption

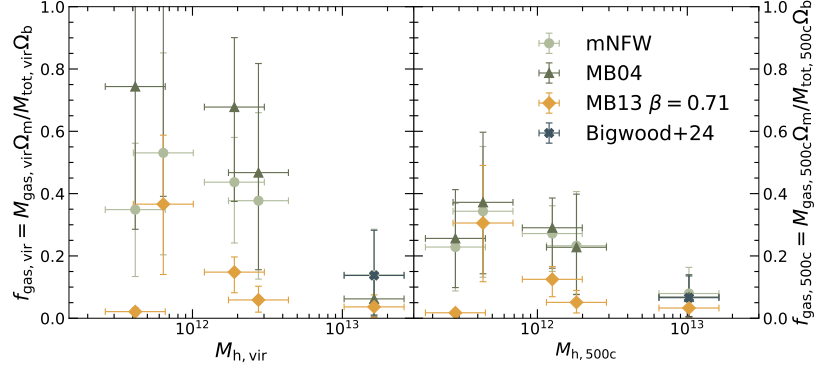


**Figure 5.** The halo gas fraction for our FRB sample plotted for a subset of the profiles considered. The left plot shows the gas fraction within the  $R_{\text{vir}}$ ,  $f_{\text{gas,vir}}$ , and the right shows the gas fraction within  $R_{500c}$ ,  $f_{\text{gas},500c}$ . For clarity, we only plot our fiducial profile (mNFW), and the highest and lowest predicting profiles (excluding NFW). We also plot the L. Bigwood et al. (2024) profile for FRB 20240209A to show that it is consistent.

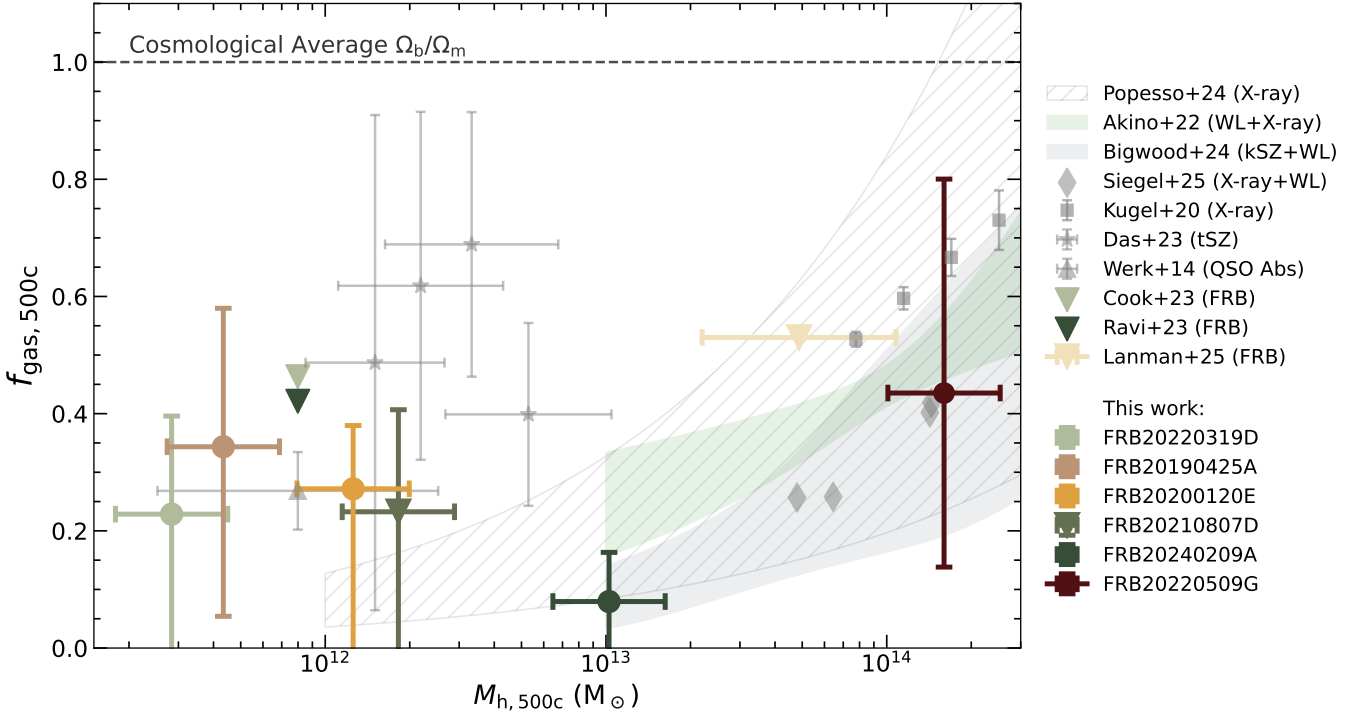


**Figure 6.** The halo gas fraction within  $R_{500c}$ ,  $f_{\text{gas},500c}$ , versus halo mass. The colored points are FRB data, including those analyzed in this work – the five FRBs in our sample plus the cluster FRB 20220509G (see text) – and measurements from the literature. For comparison, we include representative studies from the literature that use complementary observational tools; see the text for details. Note that the data in the different studies represented here are not necessarily from the same redshift.

of this profile is that cooling and precipitation of the gas is regulated by feedback processes. The above three profiles decrease the density of the gas at small radii compared to the NFW and distribute it farther out, approximating baryonic effects like feedback.

We also include the  $\beta$  model from M. J. Miller & J. N. Bregman (2013), determined empirically from X-ray data:

$$n_e(r) \propto \left(1 + \left(\frac{r}{r_c}\right)^2\right)^{-3\beta/2} \quad (11)$$

where  $\beta = 0.71$  and  $r_c = 0.35$  kpc. We assume  $r_c$  scales with  $r_s$  for different halos, but this should not affect results either way. When evaluating this profile we also consider  $\beta = 0.39$ , as indicated by more recent fits (P. Kaaret et al. 2020; Y. Zhang et al. 2024).

We further include the model of [Y. Faerman et al. \(2020\)](#). We take the tabulated fiducial model for the MW and scale to the virial radius of other halos. The shape of the model in [Y. Faerman et al. \(2017\)](#) is similar and so not included separately.

All of the above profiles are motivated by or fit to observations of the MW. Because the host of FRB20240209A is a massive elliptical, these may not generalize well. We include the “baryonification” model ([A. Schneider et al. 2019](#)), with best-fit parameters from the kinetic Sunyaev-Zeldovich effect (kSZ) study by [L. Bigwood et al. \(2024\)](#). This model alters the NFW profile in detail to emulate the observed gas distributions in X-ray observations of massive halos. For our purposes, the gas profile is:

$$\rho(r) \propto \frac{1}{\left[1 + \left(\frac{r}{0.1R_{200c}}\right)\right]^{\beta(M)} \left[1 + \left(\frac{r}{r_{ej}}\right)^\gamma\right]^{\frac{\delta-\beta(M)}{\gamma}}} \quad (12)$$

where  $\beta(M) = 3(M/M_c)^\mu/(1 + (M/M_c)^\mu)$  and  $r_{ej} = \theta_{ej}R_{200c}$ .  $M_c$ ,  $\theta_{ej}$ ,  $\delta$ ,  $\gamma$ , and  $\mu$  are the free parameters retrieved from [L. Bigwood et al. \(2024\)](#).

Given an observed  $DM_{\text{host}}$ ,  $b$ ,  $M_{\text{h,vir}}$ , and density profile,  $f_{\text{gas,vir}}$  is determined by Eqn. 7. Once  $f_{\text{gas,vir}}$  is determined for a halo, where we have assumed the DM probes out to the virial radius, we can then reintegrate the density profile to get  $f_{\text{gas,500c}}$ , the gas mass fraction within  $R_{500c}$ , which we use to compare to other observations below.  $f_{\text{gas,vir}}$  and  $f_{\text{gas,500c}}$  determined for each FRB for a subset of the profiles described above are shown in Fig. 5. There is significant scatter in  $f_{\text{gas,vir}}$ , but this is reduced in  $f_{\text{gas,500c}}$ . The FRB 20240209A measurement remains low for either definition and all of the profiles. We take the mNFW profile as our fiducial prediction, because it is roughly the median of the profiles for  $f_{\text{gas,vir}}$ . Choosing this profile results in values of  $f_{\text{gas,500c}}$  that are on the high end of the different profiles. We include the scatter in the profiles around the mNFW as additional uncertainty on our measurement. This approximates the uncertainty from our limited knowledge of the actual gas distribution.

Our fiducial measurements of  $f_{\text{gas,500c}}$  for the FRBs in our sample are plotted in Figure 6 and compared to the literature. FRB FRB20210807D is plotted as an upper limit because its non-negligible  $\tau_{\text{exc}}$  means there is likely a  $DM_{\text{host,ISM}}$  contribution (Section 2). We include the local universe cluster FRB 20220509G, discussed at the end of Section 2, in the plot to show that FRBs can probe this mass scale. The uncertainty on the mass of the corresponding cluster is 0.2dex ([X. Yang et al. 2021](#)). For this FRB, we plot the median prediction as the [L. Bigwood et al. \(2024\)](#) profile and do not include the

additional uncertainty from other profile estimates. For FRB 20230703A from [A. E. Lanman et al. \(2025\)](#), we have taken the value determined for the mNFW profile and the mass error is from the range of masses in the three groups along the FRB sightline. We plot this FRB as an upper limit because the authors did not consider  $DM_{\text{host}}$  or  $DM_{\text{cosmic}}$ . The [A. M. Cook et al. \(2023\)](#) and [V. Ravi et al. \(2025\)](#) FRB points are upper limits on the MW CGM, for which we take the DM and convert it into an  $f_{\text{gas}}$  measurement using the same procedure for the FRBs in our sample. Note that [V. Ravi et al. \(2025\)](#) uses FRB 20220319D, which is also plotted separately for our sample. For the COS-Halos quasar absorption line study (QSO Abs) ([J. K. Werk et al. 2014](#)), we have translated their limits on the cool mass of the CGM to  $R_{500c}$  using their best fit surface mass profile and plotted them for a MW sized halo. The mass error represents very roughly the scatter in halo masses in their sample. Note that because this study traces only the cool phase of the CGM it is plotted as a lower limit. For [S. Das et al. \(2023\)](#), we convert their  $M_{\text{gas,200c}}$  measurement for stellar mass bins of width 0.3dex to  $M_{\text{gas,500c}}$  using their generalized NFW profile. For [P. Popesso et al. \(2024\)](#) we use their best fit  $f_{\text{gas,500c}}$  power-law, and for [D. Akino et al. \(2022\)](#) we use the best fit evaluated at  $z = 0$ . For [L. Bigwood et al. \(2024\)](#) and [J. Siegel et al. \(2025\)](#) we take their  $M_{\text{gas,500c}}$  data and convert using our assumed cosmology. [R. Kugel et al. \(2023\)](#) is plotted as given.

As seen in Figure 6, FRBs can constrain the gas content in a wide range of halo masses. We compare FRBs as a probe of halo gas to other observational tools in Section 4.1. The FRB 20240209A measurement is the strongest, and quite low compared to other observations. We interpret this as evidence for strong AGN feedback in halos of this mass, and discuss this in Sections 4.1 and 4.2.

### 3.3. $f_{\text{CGM}}$

Once we have determined  $f_{\text{gas}}$  for a range of halo masses, it is interesting to consider what this implies about the cosmological baryon budget. In particular, we can use our measurements to determine  $f_{\text{CGM}} \equiv \Omega_{\text{CGM}}/\Omega_b$  by integrating over the halo mass function (MF). Recently, [L. Connor et al. \(2025\)](#) provided a full accounting of the Universe’s baryons, including the “missing” baryons of the IGM and CGM. They used FRBs to determine  $f_{\text{IGM}}$ , but  $f_{\text{CGM}}$  was determined indirectly by constraining other baryonic components (e.g. the ICM with X-rays) and requiring the sum of all components to reach  $\Omega_b$ . They found  $f_{\text{CGM}} = 0.08^{+0.07}_{-0.06}$  for halos of mass  $10^9 - 5 \times 10^{12} M_\odot$ . Using the tinker08 MF in COLOSSUS ([J. Tinker et al. 2008](#)) and a weighted

average of  $f_{\text{gas,vir}}$  for our 4 FRBs within the same mass range, we find  $f_{\text{CGM}} = 0.11 \pm 0.07$ . Thus we extend the ability of FRBs to account for the missing baryons beyond just the IGM. We have seen that FRBs can also constrain gas in the group and cluster scale halos (Figure 6), so in principle FRBs alone can account for all components of the diffuse ionized gas in the Universe.

## 4. DISCUSSION

### 4.1. Comparison to other probes

Because the DM is a simple integral of the electron density  $n_e$ , FRBs do not suffer from some of the limitations of other gas probes. This comes at the cost of a single line of sight through a halo per FRB. We have shown that FRBs can measure gas in halos of mass  $\sim 10^{11-13} M_\odot$  (Section 3.2). While FRBs have been shown to preferentially occur in massive star-forming galaxies (K. Sharma et al. 2024), at least three known FRBs have dwarf host galaxies (S. P. Tendulkar et al. 2017; S. Bhandari et al. 2020; D. M. Hewitt et al. 2024). Similarly, the existence of a few FRBs with massive cluster hosts, including FRB 20220509G, indicates that future FRBs could be discovered in the most massive systems (up to  $\sim 10^{15} M_\odot$ ). So a large sample of localized FRBs can in principle constrain the gas content of halos of all sizes.

This is in contrast to the other probes (the k/tSZ effect, absorption line studies, and X-rays) which can be seen in the representative works that we have plotted in Figure 6. The tSZ effect is  $\propto n_e T_e$ , both of which depend broadly on the halo mass, so that it is difficult to detect for low to intermediate mass halos. The state-of-the-art measurements are highly uncertain for MW mass halos and below (S. Das et al. 2023, 2025). The kSZ signal also depends on the halo mass ( $\propto n_e v$ , where  $v$  is set by large-scale structure), and the signal is intrinsically faint such that it can only be measured down to  $10^{13} M_\odot$  with current instruments (L. Bigwood et al. 2024). The quasar absorption line studies probe only the cool and warm phases of the CGM ( $\lesssim 10^6$  K), and so cannot in general study the gas of large groups and clusters (J. Tumlinson et al. 2017). Finally, the X-ray signal ( $\propto n_e^2$ ) is also strongest in the most massive systems. Recent eROSITA results have pushed down to  $\sim 10^{12.5} M_\odot$  (P. Popesso et al. 2024; Y. Zhang et al. 2024).

Another interesting detail to note is that we have shown that FRBs can measure individual halos. The kSZ effect, for example, is measured statistically. Similarly, FRB analyses up to this point have focused on statistical measurements of baryonic feedback (e.g. the  $p(\text{DM}|z)$  relationship R. Reischke & S. Hagstotz (2025)). This makes our method interesting on a per-source as-

trophysical level and a good complement to other FRB analyses. On the other hand, because we have only measured the gas in a handful of individual halos, we need a larger sample to make definitive claims. We can expect a larger sample in the near future (Section 4.5).

Because of the small sample size and the relatively large errors (Figure 6), we cannot make broad conclusions when comparing the FRB data to the literature. For FRBs 20200120E and 20210807D, the errors are large enough to be consistent with all of the tSZ, X-ray, and absorption line data (S. Das et al. 2023; P. Popesso et al. 2024; J. K. Werk et al. 2014). However, the FRB 20240209A measurement is less uncertain and quite low. It appears to be slightly in tension with both the pre-eROSITA X-ray measurements (D. Akino et al. 2022) and possibly the high-mass end of the tSZ sample from (S. Das et al. 2023). We note that the measurement is consistent with the eROSITA X-ray measurements (P. Popesso et al. 2024; Y. Zhang et al. 2024).

A small gas fraction at the group scale implies stronger baryonic feedback and a stronger suppression of the matter power spectrum. This is expected in a stronger AGN feedback scenario, which we discuss in the next section. When taken together, the four low mass measurements (FRBs 20210807D, 20200120E, and 20190425A) indicate that  $f_{\text{gas}}$  may break from the decreasing trend that is seen when moving down in mass from  $M_h \sim 10^{15} M_\odot$  to  $\sim 10^{12.5} M_\odot$ . This is in agreement with other observables (J. K. Werk et al. (2014), S. Das et al. (2023)) and the interpretation that  $L_*$  galaxies retain a larger fraction of their baryons than massive galaxies and galaxy groups due to the prevalence of AGN feedback in the latter. More data is required to confirm this trend.

### 4.2. FRB 20240209A - AGN feedback

The FRB data indicates that there is little gas in the host of FRB 20240209A. It is expected that halos of mass  $\sim 10^{13} M_\odot$  will be strongly affected by AGN feedback, which can push baryons out to the virial radius or beyond and prevent further accretion (I. G. McCarthy et al. 2010; B. D. Oppenheimer et al. 2021). This process creates the quenched elliptical galaxies we see in the local universe, such as the host of FRB 20240209A (V. Springel et al. 2005). Our measurement of  $\text{DM}_{\text{host,CGM}}$  in the host of FRB 20240209A aligns most closely with the SIMBA simulation (Figure 4), which has a stronger AGN feedback implementation than IllustrisTNG, but is consistent with both within the uncertainty. It is further completely inconsistent with the SIMBA simulation with AGN feedback turned off. When converted to a measurement of  $f_{\text{gas}}$  (Figure 6), it is most consistent with the findings of L. Bigwood et al. (2024), which favor

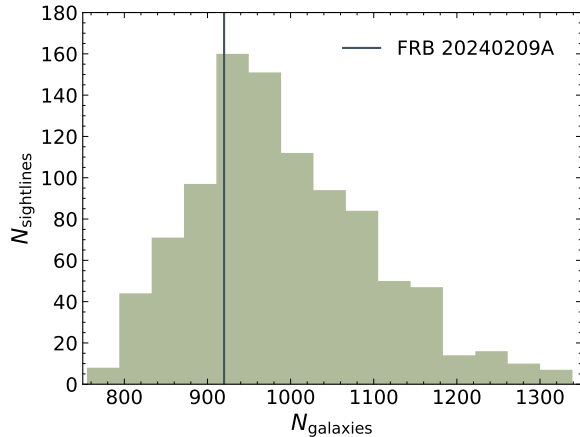


**Figure 7.** The number of galaxies within 5 Mpc of the sightline to FRB 20240209A compared to the distribution for 1000 random sightlines following the procedure of [M. Hussaini et al. \(2025\)](#). The FRB 20240209A sightline is consistent with the median overdensity of foreground galaxies to this redshift.

a stronger AGN feedback scenario. Below we discuss further evidence in support of the interpretation that AGN feedback has evacuated the host of FRB 20240209A.

First, we note that the low  $\text{DM}_{\text{host,CGM}}$  could be explained by sightline-to-sightline variance in the DM components. While this should be captured in our uncertainty estimates, we check that the sightline to FRB 20240209A is not underdense, leading to a low  $\text{DM}_{\text{cosmic}}$ . To do this we follow the procedure of [M. Hussaini et al. \(2025\)](#). We use the photometric redshift catalog of [R. Beck et al. \(2022\)](#), which combines Pan-STARRS and Wide-field Infrared Survey Explorer (WISE) data. We count the number of galaxies in a 5 Mpc cylinder towards FRB 20240209A and 1000 random sightlines within 5 degrees of galactic latitude. The number of galaxies in each sightline is plotted in Figure 7. The sightline to FRB 20240209A is only slightly underdense, so this is unlikely to explain the low  $\text{DM}_{\text{host,CGM}}$  measurement. On the other hand, we have not accounted for sightline-to-sightline variance in the CGM of the host galaxies themselves when converting  $\text{DM}_{\text{host,CGM}}$  to  $f_{\text{gas}}$ . This variance is captured in the curves calculated for the simulation halos (Figure 4), and appears to be roughly 50% including halo-to-halo variance. This is similar to the 0.2dex uncertainty we assumed for  $\text{DM}_{\text{MW,CGM}}$ . This uncertainty is not enough to significantly change our conclusions. Finally we check the local environment around the host of FRB 20240209A, as central galaxies in groups or clusters often host AGN: we find only a minor overdensity within 5 Mpc around the host compared to the average density in the catalog at this redshift, and

only one galaxy closer than 3 Mpc, so the galaxy is likely not part of a group.

Next, we consider the available information about the host of FRB 20240209A from multiwavelength data. The host is analyzed in detail in [T. Eftekhar et al. \(2025\)](#). Using a deep Gemini spectrum and SED fitting, they find strong evidence that the host is a quenched elliptical. In particular, the very low star formation rate (SFR) ( $< 0.36 M_{\odot} \text{ yr}^{-1}$ ), which is apparent in the lack of emission lines in the spectrum, combined with the high stellar mass places the host securely below the star forming main sequence (the specific SFR (sSFR) is  $\log_{10}\text{sSFR} < -11.8$ ). The stellar population age inferred from SED fitting is  $t_m \sim 11 \text{ Gyr}$ , and indicates most of the stellar mass was formed around this time. Further, the host is squarely in the elliptical region of the WISE color diagram. Combined with the very low gas content of the halo inferred from the FRB in this work, the obvious interpretation is that this galaxy has been quenched by a period of strong AGN feedback after  $z \sim 2$ . However, the WISE colors do not classify the host as an AGN, indicating the lack of a dusty torus. There is also a lack of any obvious optical emission lines associated with AGN activity. This seems to indicate that the nuclear supermassive black hole is not currently active or in a low power state.

Another piece of information that was not examined in detail by [T. Eftekhar et al. \(2025\)](#) is the radio detection of the host by [C. J. Law et al. \(2024\)](#). An unresolved source coincident with the host was observed at 1-2 GHz with the VLA. The resolution is not sufficient to definitively associate the radio source with the nucleus of the host galaxy. However, if we assume that the radio emission in the host is entirely synchrotron from star formation, using the radio luminosity-SFR relation gives a  $\text{SFR} \sim 5 M_{\odot} \text{ yr}^{-1}$  ([E. J. Murphy et al. 2011](#)). This is an order of magnitude above the SFR inferred from the optical and infrared data, implying that there is a significant contribution to the radio emission from an AGN. A simple power-law fit to the flux densities gives a spectral index of  $\alpha = -1.84$  ( $S \propto \nu^{\alpha}$ , where  $S$  is the flux density and  $\nu$  is frequency). This is steeper than expected from either star formation or an active radio-loud AGN. The steep spectral index may be consistent with an aged synchrotron population, for example if a past AGN has become dormant and is now producing less relativistic electrons.

Based on the above discussion, we conclude that our measurement of a small  $f_{\text{gas}}$  in the host of FRB 20240209A is likely due to AGN feedback in the host galaxy that quenched star formation and expelled gas. The AGN may have since turned off or entered a low-

power state. Thus we show that FRBs can measure feedback in individual halos, opening a new pathway to understanding baryonic effects.

#### 4.3. FRB 20240209A - Host galaxy association

FRB 20240209A is significantly offset from its host elliptical galaxy (V. Shah et al. 2025). It is therefore worth asking if the FRB is associated with the putative host. The FRB is unlikely to be in a background galaxy, due to the asymmetry of cosmic DM (L. Connor et al. 2025) and the tight total DM budget of this source. If it were, the CGM constraints would be even more significant because it would have more IGM DM and double the path length through the host galaxy's halo. Thus, the failure mode of our analysis is if the FRB is actually in the foreground of this galaxy. This is unlikely given the depth of optical imaging at the position of the FRB and the relative low redshift of the elliptical. No galaxy has been detected down to  $r \approx 25.9$  mag (3- $\sigma$ ), ruling out galaxies with luminosity above  $5 \times 10^6 L_\odot$  that are halfway to the elliptical host candidate. Furthermore, elliptical galaxies are known to have far more globular clusters than late-type galaxies of similar mass. FRB 20200120E, which is also in our sample, resides in a globular cluster of M81, providing precedent for large host offsets. As in the discovery papers (V. Shah et al. 2025; T. Eftekhari et al. 2025), we conclude that FRB 20240209A is indeed in the outskirts of the massive elliptical, whether in a globular cluster or offset due to the progenitor's advanced stellar age.

#### 4.4. The Milky Way Halo

One of the most uncertain aspects of our analysis is  $DM_{MW,CGM}$ .  $DM_{MW,CGM}$  is dominated by a hot volume-filling gas phase, which is currently best measured in the X-ray (S. Das et al. 2020). In principle, OVII measurements correlate with the DM (J. X. Prochaska & Y. Zheng 2019; S. Das et al. 2020), which could allow independent constraints on this component. However, the uncertainty on OVII column measurements from X-ray absorption is very high, and the number of sightlines is limited (e.g. T. Fang et al. (2015)). The YT20 model fits X-ray EM data; however, the model includes a spherical and “disk”-like component, only the latter of which is fit to the data (S. Yamasaki & T. Totani 2020). The spherical component assumes an  $f_{\text{gas}}$  for the MW, and dominates high galactic latitude sightlines. Further, there is likely significant sightline-to-sightline variance in  $DM_{MW,CGM}$ , given the large scatter in the measurements of both S. Das et al. (2020) and S. Yamasaki & T. Totani (2020). Finally, there are a large number of models in the literature for the halo

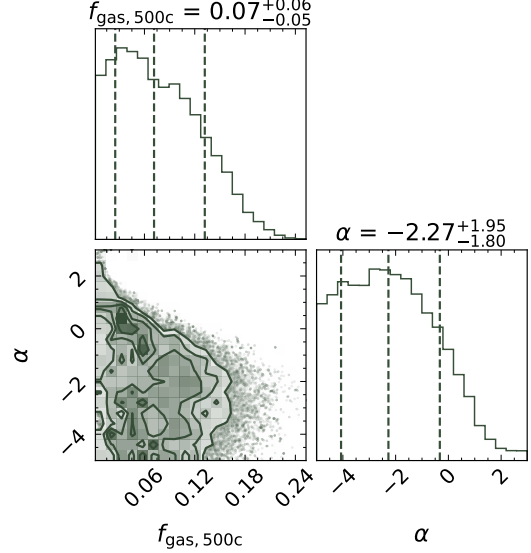


**Figure 8.** Corner plot of the MCMC fit to our FRB sample.  $\alpha$  is the inner power-law slope of the CGM radial profile. The sample is not large enough for a good constraint on  $\alpha$ , but the fit demonstrates that there is constraining power in the data that can be taken advantage of with a future larger sample.

gas distribution, which produce widely varying predictions for  $DM_{MW,CGM}$  (J. X. Prochaska & Y. Zheng 2019; L. C. Keating & U.-L. Pen 2020).

We wish to be conservative for our estimate of  $DM_{MW,CGM}$ . S. Das et al. (2020) provides a comprehensive compilation of data on all phases of the MW CGM and converts these to DM estimates. These estimates are on average twice as high as those from YT20. Similarly, J. Hoffmann et al. (2026) find an average  $DM_{MW,CGM}$  roughly twice as large as the YT20 model, and Y. Liu et al. (2026) find that the average  $DM_{MW,CGM}$  can significantly exceed the YT20 model average for portions of the sky. Thus we take the YT20 model as our conservative estimate. We include a scatter of 0.2 dex to capture sightline-to-sightline variance. We emphasize that a factor of 2 increase in  $DM_{MW,CGM}$  would lead to a negligible  $DM_{\text{host},CGM}$  in most cases. This would make the constraints on  $DM_{\text{host},CGM}$  more severe, strengthening the conclusions of this work. On the other hand, if  $DM_{MW,CGM}$  were 50% of our assumed values, this would add just  $\sim 15 \text{ pc cm}^{-3}$  to inferred host CGM.

#### 4.5. Looking ahead - All-Sky Monitors

Our method for measuring the CGM in extragalactic halos relies on two characteristics of the FRB sample: low redshift, such that the CGM signal is not washed out by  $DM_{\text{cosmic}}$ , and negligible  $DM_{\text{host},ISM}$ . The lat-

ter cannot be predicted, and merely requires a large enough sample such that a good number of FRBs originated from favorable environments (outside the disk, for example). However, with a large enough sample, a  $DM_{host,ISM}$  component could be fit simultaneously to the data. For the former, a large sample of local universe FRBs is expected from upcoming all-sky monitors. The mean distance of an observed sample of FRBs scales as the  $1/\sqrt{S_{min}}$ , where  $S_{min}$  is the minimum detectable flux of the survey (D. Li et al. 2019). All-sky, modest sensitivity telescopes will preferentially discover bright, nearby FRBs with small DM contributions from the IGM. A large FOV is easily achieved at radio frequencies with aperture arrays. This fact will be taken advantage of by the Coherent All-Sky Monitor (CASM) (Connor et al. in prep) and similar projects (BURSTT; H.-H. Lin et al. (2022) and CHARTs in Chile) to discover a large number of local universe FRBs. CASM is expected to find order  $10^2$  local universe FRBs each year. A sample of this size could be used to build upon the work presented in this paper, potentially discriminating between feedback scenarios in simulations and pinning down the trend in  $f_{\text{gas}}$  across halo masses.

The FRB data also encodes information about the radial profile of the CGM through the different  $b_{\perp}$  of the FRBs. Feedback determines the radial profile; stronger feedback will push baryons farther out of the halo, producing a flatter profile. Further, the distribution of gas on these scales determines the suppression of the matter power spectrum, which can be significant for  $10^{12-13} M_{\odot}$  halos (S. N. B. Debackere et al. 2019). With a large sample, it will be possible to fit both the normalization,  $f_{\text{gas}}$ , and the shape of the CGM, ideally in mass bins. To demonstrate this, we use Markov Chain Monte Carlo (MCMC) to fit a global  $f_{\text{gas},500c}$  and inner CGM power law slope  $\alpha$  to our sample of five FRBs. The radial profile is parameterized with  $\alpha$  as

$$\rho(r) \propto \frac{1}{y^{\alpha}(y_0 + y)^{3-\alpha}}, \quad (13)$$

so that  $\alpha$  represents the inner slope of the profile and the profile converges to the standard NFW at large radii where we do not have data. We chose  $y_0 = 2$  as in the mNFW profile, so that all of the FRBs are originating from radii smaller than the transition between the inner and outer slopes. We use uniform priors on both parameters. Our sample is small and may be biased by individual FRBs; however, this analysis serves to demonstrate the methodology. The results of the fit are shown in Figure 8. Clearly a larger sample is necessary for a good determination of  $\alpha$ , but the fit demonstrates that there is constraining power in the data. Interestingly,

the data prefer a rising inner CGM profile, but a larger sample is required to verify this. The best fit  $f_{\text{gas},500c}$  is likely heavily influenced by FRB 20240209A, which we expect to give a much tighter constraint than the other FRBs (Figure 6), and is not 1-1 comparable to our other measurements because of the different profile.

A large sample of local universe FRBs will also enable a better characterization of the MW CGM. Beyond simply the total integrated DM of the MW halo, it will be interesting and feasible to look for deviations from spherical symmetry. The largest will be due to the large and small Magellanic clouds, and the M31 halo (if this is not counted separately from the MW halo). We can likely expect each of these to contribute tens of  $\text{pc cm}^{-3}$  to the DM in their respective directions (J. X. Prochaska & Y. Zheng 2019). Thus a first target will be a dipole asymmetry between the northern and southern galactic hemispheres. The recent work by Y. Liu et al. (2026) claims to have detected a dipole anisotropy in the MW CGM in galactic longitude, but more work is required to verify. Furthermore, the X-ray data on the MW suggest that there is a significant disk-like component to the CGM, distinct from the hot volume-filling phase (S. Yamasaki & T. Totani 2020). This component likely makes up a significant fraction of the total CGM DM, but separating out its directional dependence will require a large sample. Finally, recent work indicates that the stellar and dark matter components of the MW halo are ellipsoidal and tilted with respect to the stellar disk (J. J. Han et al. 2022a,b). It would be interesting to determine what impact, if any, this has on the gas distribution in the halo. Several hundred local universe FRB sightlines from CASM is an important prerequisite for this science.

## 5. CONCLUSION

In this work we have used FRBs to study the CGM of their host galaxies. We use local universe FRBs ( $z < 0.2$ ), so that the contribution to the DM from the cosmic web does not dominate the contribution from the host galaxy. We select a sample of five FRBs based on their scattering timescales, rotation measures, host galaxy inclinations, and impact parameters. These FRBs likely have a negligible DM contribution from the host ISM and circumburst medium. We isolate the DM of the host CGM by robustly estimating the DM of the MW and the cosmic web along each sightline. We compare these values to simulations and convert them to measurements of the gas content of the host halos. Our main findings are:

- FRBs can measure the gas in halos of mass  $10^{11-13} M_{\odot}$ , and up to  $\sim 10^{14} M_{\odot}$  with a larger sample including cluster hosts. In contrast, other

observables of diffuse gas are limited in the mass ranges they can probe. Constraining the gas content in a wide range of halo masses is important for understanding baryonic feedback.

- The massive elliptical host galaxy of FRB 20240209A is extremely gas poor ( $M_{\text{gas,vir}} = 0.02^{+0.02}_{-0.02} M_{\text{h,vir}}$ ). Considering multiwavelength data of the host, we find evidence that the gas was expelled by a period of strong AGN feedback. This measurement effectively rules out a no AGN feedback scenario by being in strong tension with the SIMBA simulation with AGN feedback turned off. It also aligns more closely with studies using other observables (X-ray, kSZ) that find strong AGN feedback scenarios.
- The other four FRBs in our sample are broadly consistent with simulations. They hint at a trend of increasing  $f_{\text{gas}}$  when moving to lower mass halos

from  $M_{\text{h}} \sim 10^{13}$ , which is expected from AGN feedback affecting the highest mass galaxies.

- Upcoming aperture array all-sky monitors, such as CASM, will uncover a large number of local universe FRBs suitable for this science. With a larger sample, we will be able to discriminate between AGN feedback implementations in simulations and determine the trend in  $f_{\text{gas}}$  with halo mass to better precision. We will also be able to constrain the radial profile of the gas and the gas in the MW halo. This opens a promising new path to understanding feedback with FRBs.

## ACKNOWLEDGMENTS

SM thanks Will Golay for a helpful discussion about radio spectra.

*Software:* astropy ( Astropy Collaboration et al. 2013, 2018, 2022), COLOSSUS (B. Diemer 2018), emcee (D. Foreman-Mackey et al. 2013), yt (M. J. Turk et al. 2011), corner (D. Foreman-Mackey 2016)

## REFERENCES

Ade, P. A. R., Aghanim, N., Arnaud, M., et al. 2016, *Astronomy & Astrophysics*, 594, A13, doi: [10.1051/0004-6361/201525830](https://doi.org/10.1051/0004-6361/201525830)

Akino, D., Eckert, D., Okabe, N., et al. 2022, *Publications of the Astronomical Society of Japan*, 74, 175, doi: [10.1093/pasj/psab115](https://doi.org/10.1093/pasj/psab115)

Anna-Thomas, R., Law, C. J., Koch, E. W., et al. 2025, *The Astrophysical Journal*, 993, 221, doi: [10.3847/1538-4357/ae1014](https://doi.org/10.3847/1538-4357/ae1014)

Astropy Collaboration, Robitaille, T. P., Tollerud, E. J., et al. 2013, *A&A*, 558, A33, doi: [10.1051/0004-6361/201322068](https://doi.org/10.1051/0004-6361/201322068)

Astropy Collaboration, Price-Whelan, A. M., Sipőcz, B. M., et al. 2018, *AJ*, 156, 123, doi: [10.3847/1538-3881/aabc4f](https://doi.org/10.3847/1538-3881/aabc4f)

Astropy Collaboration, Price-Whelan, A. M., Lim, P. L., et al. 2022, *ApJ*, 935, 167, doi: [10.3847/1538-4357/ac7c74](https://doi.org/10.3847/1538-4357/ac7c74)

Beck, R., Dodds, S. C., & Szapudi, I. 2022, *Monthly Notices of the Royal Astronomical Society*, 515, 4711, doi: [10.1093/mnras/stac1714](https://doi.org/10.1093/mnras/stac1714)

Behroozi, P., Wechsler, R. H., Hearn, A. P., & Conroy, C. 2019, *Monthly Notices of the Royal Astronomical Society*, 488, 3143, doi: [10.1093/mnras/stz1182](https://doi.org/10.1093/mnras/stz1182)

Berkhuijsen, E. M., Mitra, D., & Müller, P. 2006, *Astronomische Nachrichten*, 327, 82–96, doi: [10.1002/asna.200510488](https://doi.org/10.1002/asna.200510488)

Bhandari, S., Sadler, E. M., Prochaska, J. X., et al. 2020, *The Astrophysical Journal Letters*, 895, L37, doi: [10.3847/2041-8213/ab672e](https://doi.org/10.3847/2041-8213/ab672e)

Bhardwaj, M., Lee, J., & Ji, K. 2024, Selection bias obfuscates the discovery of fast radio burst sources, <https://arxiv.org/abs/2408.01876>

Bhardwaj, M., Gaensler, B. M., Kaspi, V. M., et al. 2021, *The Astrophysical Journal Letters*, 910, L18, doi: [10.3847/2041-8213/abeaa6](https://doi.org/10.3847/2041-8213/abeaa6)

Bhardwaj, M., Michilli, D., Kirichenko, A. Y., et al. 2023, Host Galaxies for Four Nearby CHIME/FRB Sources and the Local Universe FRB Host Galaxy Population, <https://arxiv.org/abs/2310.10018>

Bigwood, L., Amon, A., Schneider, A., et al. 2024, Weak lensing combined with the kinetic Sunyaev Zel'dovich effect: A study of baryonic feedback, <https://arxiv.org/abs/2404.06098>

Cen, R., & Ostriker, J. P. 1999, *ApJ*, 514, 1, doi: [10.1086/306949](https://doi.org/10.1086/306949)

Chambers, K. C., Magnier, E. A., Metcalfe, N., et al. 2019, The Pan-STARRS1 Surveys, <https://arxiv.org/abs/1612.05560>

Connor, L., & Ravi, V. 2022, *Nature Astronomy*, 6, 1035, doi: [10.1038/s41550-022-01719-7](https://doi.org/10.1038/s41550-022-01719-7)

Connor, L., van Leeuwen, J., Oostrum, L. C., et al. 2020, *MNRAS*, 499, 4716, doi: [10.1093/mnras/staa3009](https://doi.org/10.1093/mnras/staa3009)

Connor, L., Ravi, V., Catha, M., et al. 2023, *The Astrophysical Journal Letters*, 949, L26, doi: [10.3847/2041-8213/acd3ea](https://doi.org/10.3847/2041-8213/acd3ea)

Connor, L., Ravi, V., Sharma, K., et al. 2025, *Nature Astronomy*, 9, 1226, doi: [10.1038/s41550-025-02566-y](https://doi.org/10.1038/s41550-025-02566-y)

Cook, A. M., Bhardwaj, M., Gaensler, B. M., et al. 2023, *The Astrophysical Journal*, 946, 58, doi: [10.3847/1538-4357/acbbd0](https://doi.org/10.3847/1538-4357/acbbd0)

Cordes, J. M., & Chatterjee, S. 2019, *Annual Review of Astronomy and Astrophysics*, 57, 417–465, doi: [10.1146/annurev-astro-091918-104501](https://doi.org/10.1146/annurev-astro-091918-104501)

Cordes, J. M., & Lazio, T. J. W. 2003, NE2001.I. A New Model for the Galactic Distribution of Free Electrons and its Fluctuations, <https://arxiv.org/abs/astro-ph/0207156>

Das, S., Chiang, Y.-K., & Mathur, S. 2023, *The Astrophysical Journal*, 951, 125, doi: [10.3847/1538-4357/acd764](https://doi.org/10.3847/1538-4357/acd764)

Das, S., Mathur, S., Gupta, A., Nicastro, F., & Krongold, Y. 2020, *Monthly Notices of the Royal Astronomical Society*, 500, 655, doi: [10.1093/mnras/staa3299](https://doi.org/10.1093/mnras/staa3299)

Das, S., Truong, N., Chiang, Y.-K., & Mathur, S. 2025, *The Astrophysical Journal*, 991, 205, doi: [10.3847/1538-4357/adfdd6](https://doi.org/10.3847/1538-4357/adfdd6)

Davé, R., Anglés-Alcázar, D., Narayanan, D., et al. 2019, *Monthly Notices of the Royal Astronomical Society*, 486, 2827–2849, doi: [10.1093/mnras/stz937](https://doi.org/10.1093/mnras/stz937)

Debackere, S. N. B., Schaye, J., & Hoekstra, H. 2019, *Monthly Notices of the Royal Astronomical Society*, 492, 2285, doi: [10.1093/mnras/stz3446](https://doi.org/10.1093/mnras/stz3446)

Diemer, B. 2018, *ApJS*, 239, 35, doi: [10.3847/1538-4365/aaee8c](https://doi.org/10.3847/1538-4365/aaee8c)

Diemer, B., & Joyce, M. 2019, *ApJ*, 871, 168, doi: [10.3847/1538-4357/aafad6](https://doi.org/10.3847/1538-4357/aafad6)

Eftekhari, T., Dong, Y., Fong, W., et al. 2025, *The Astrophysical Journal Letters*, 979, L22, doi: [10.3847/2041-8213/ad9de2](https://doi.org/10.3847/2041-8213/ad9de2)

Faerman, Y., Sternberg, A., & McKee, C. F. 2017, *ApJ*, 835, 52, doi: [10.3847/1538-4357/835/1/52](https://doi.org/10.3847/1538-4357/835/1/52)

Faerman, Y., Sternberg, A., & McKee, C. F. 2020, *The Astrophysical Journal*, 893, 82, doi: [10.3847/1538-4357/ab7ff](https://doi.org/10.3847/1538-4357/ab7ff)

Fang, T., Buote, D., Bullock, J., & Ma, R. 2015, *The Astrophysical Journal Supplement Series*, 217, 21, doi: [10.1088/0067-0049/217/2/21](https://doi.org/10.1088/0067-0049/217/2/21)

Foreman-Mackey, D. 2016, *The Journal of Open Source Software*, 1, 24, doi: [10.21105/joss.00024](https://doi.org/10.21105/joss.00024)

Foreman-Mackey, D., Hogg, D. W., Lang, D., & Goodman, J. 2013, *Publications of the Astronomical Society of the Pacific*, 125, 306–312, doi: [10.1086/670067](https://doi.org/10.1086/670067)

Gordon, A. C., Fong, W.-f., Kilpatrick, C. D., et al. 2023, *ApJ*, 954, 80, doi: [10.3847/1538-4357/ace5aa](https://doi.org/10.3847/1538-4357/ace5aa)

Guachalla, B. R., Schaan, E., Hadzhiyska, B., et al. 2025, *Physical Review D*, 112, doi: [10.1103/lqbj-wcqj](https://doi.org/10.1103/lqbj-wcqj)

Haffner, L. M., Reynolds, R. J., Tufte, S. L., et al. 2003, *The Astrophysical Journal Supplement Series*, 149, 405, doi: [10.1086/378850](https://doi.org/10.1086/378850)

Han, J. J., Conroy, C., Johnson, B. D., et al. 2022a, *The Astronomical Journal*, 164, 249, doi: [10.3847/1538-3881/ac97e9](https://doi.org/10.3847/1538-3881/ac97e9)

Han, J. J., Naidu, R. P., Conroy, C., et al. 2022b, *The Astrophysical Journal*, 934, 14, doi: [10.3847/1538-4357/ac795f](https://doi.org/10.3847/1538-4357/ac795f)

Harris, W. E. 2009, *The Astrophysical Journal*, 703, 939, doi: [10.1088/0004-637X/703/1/939](https://doi.org/10.1088/0004-637X/703/1/939)

He, C., Ng, C.-Y., & Kaspi, V. M. 2013, *The Astrophysical Journal*, 768, 64, doi: [10.1088/0004-637X/768/1/64](https://doi.org/10.1088/0004-637X/768/1/64)

Hewitt, D. M., Bhardwaj, M., Gordon, A. C., et al. 2024, *The Astrophysical Journal Letters*, 977, L4, doi: [10.3847/2041-8213/ad8ce1](https://doi.org/10.3847/2041-8213/ad8ce1)

HI4PI Collaboration:, Ben Bekhti, N., Flöer, L., et al. 2016, *A&A*, 594, A116, doi: [10.1051/0004-6361/201629178](https://doi.org/10.1051/0004-6361/201629178)

Hoffmann, J., James, C., Prochaska, J. X., & Glowacki, M. M. 2026, I can see your halo: Constraining the Milky Way halo DM with FRB population studies, <https://arxiv.org/abs/2601.05496>

Hussaini, M., Connor, L., Konietzka, R. M., et al. 2025, *The Astrophysical Journal Letters*, 993, L27, doi: [10.3847/2041-8213/ae0a49](https://doi.org/10.3847/2041-8213/ae0a49)

Ivezic, Z., Kahn, S. M., Tyson, J. A., et al. 2019, *The Astrophysical Journal*, 873, 111, doi: [10.3847/1538-4357/ab042c](https://doi.org/10.3847/1538-4357/ab042c)

Kaaret, P., Koutroumpa, D., Kuntz, K. D., et al. 2020, *Nature Astronomy*, 4, 1072–1077, doi: [10.1038/s41550-020-01215-w](https://doi.org/10.1038/s41550-020-01215-w)

Keating, L. C., & Pen, U.-L. 2020, *Monthly Notices of the Royal Astronomical Society: Letters*, 496, L106–L110, doi: [10.1093/mnrasl/slaa095](https://doi.org/10.1093/mnrasl/slaa095)

Khrykin, I. S., Ata, M., Lee, K.-G., et al. 2024, *The Astrophysical Journal*, 973, 151, doi: [10.3847/1538-4357/ad6567](https://doi.org/10.3847/1538-4357/ad6567)

Kirsten, F., Marcote, B., Nimmo, K., et al. 2022, *Nature*, 602, 585–589, doi: [10.1038/s41586-021-04354-w](https://doi.org/10.1038/s41586-021-04354-w)

Konietzka, R. M., Connor, L., Semenov, V. A., et al. 2025, Ray-tracing Fast Radio Bursts Through IllustrisTNG: Cosmological Dispersion Measures from Redshift 0 to 5.5, <https://arxiv.org/abs/2507.07090>

Kugel, R., Schaye, J., Schaller, M., et al. 2023, *Monthly Notices of the Royal Astronomical Society*, 526, 6103, doi: [10.1093/mnras/stad2540](https://doi.org/10.1093/mnras/stad2540)

Lanman, A. E., Simha, S., Masui, K. W., et al. 2025, Constraining Baryon Fractions in Galaxy Groups and Clusters with the First CHIME/FRB Outrigger, <https://arxiv.org/abs/2509.07097>

Law, C. J., Bhardwaj, M., Burke-Spolaor, S., et al. 2024, *The Astronomer's Telegram*, 16701, 1

Law, C. J., Sharma, K., Ravi, V., et al. 2024, *The Astrophysical Journal*, 967, 29, doi: [10.3847/1538-4357/ad3736](https://doi.org/10.3847/1538-4357/ad3736)

Lee, K.-G., Khrykin, I. S., Simha, S., et al. 2023, *ApJL*, 954, L7, doi: [10.3847/2041-8213/acefb5](https://doi.org/10.3847/2041-8213/acefb5)

Leung, C., Borrow, J., Masui, K. W., et al. 2025a, Nulling baryonic feedback in weak lensing surveys using cross-correlations with fast radio bursts, <https://arxiv.org/abs/2509.19514>

Leung, C., Simha, S., Medlock, I., et al. 2025b, Stellar Mass-Dispersion Measure Correlations Constrain Baryonic Feedback in Fast Radio Burst Host Galaxies, <https://arxiv.org/abs/2507.16816>

Li, D., Yalinewich, A., & Breysse, P. C. 2019, arXiv e-prints, arXiv:1902.10120, doi: [10.48550/arXiv.1902.10120](https://doi.org/10.48550/arXiv.1902.10120)

Li, R.-N., Xu, K., Gao, D.-H., et al. 2025, *The Astrophysical Journal*, 989, 77, doi: [10.3847/1538-4357/adeb72](https://doi.org/10.3847/1538-4357/adeb72)

Lin, H.-H., Lin, K.-y., Li, C.-T., et al. 2022, *PASP*, 134, 094106, doi: [10.1088/1538-3873/ac8f71](https://doi.org/10.1088/1538-3873/ac8f71)

Liu, Y., Wang, B., Wu, P., Wei, J.-J., & Wu, X.-F. 2026, Investigating the Anisotropy of Dispersion Measure Contribution from the Galactic Halo by Using Fast Radio Bursts, <https://arxiv.org/abs/2601.02849>

Lorimer, D. R., Bailes, M., McLaughlin, M. A., Narkevic, D. J., & Crawford, F. 2007, *Science*, 318, 777–780, doi: [10.1126/science.1147532](https://doi.org/10.1126/science.1147532)

Luan, J., & Goldreich, P. 2014, *The Astrophysical Journal*, 785, L26, doi: [10.1088/2041-8205/785/2/l26](https://doi.org/10.1088/2041-8205/785/2/l26)

Macquart, J.-P., Prochaska, J. X., McQuinn, M., et al. 2020, *Nature*, 581, 391–395, doi: [10.1038/s41586-020-2300-2](https://doi.org/10.1038/s41586-020-2300-2)

Maller, A. H., & Bullock, J. S. 2004, *MNRAS*, 355, 694, doi: [10.1111/j.1365-2966.2004.08349.x](https://doi.org/10.1111/j.1365-2966.2004.08349.x)

Manchester, R. N., Hobbs, G. B., Teoh, A., & Hobbs, M. 2005, *The Astronomical Journal*, 129, 1993–2006, doi: [10.1086/428488](https://doi.org/10.1086/428488)

Marinacci, F., Vogelsberger, M., Pakmor, R., et al. 2018, *Monthly Notices of the Royal Astronomical Society*, doi: [10.1093/mnras/sty2206](https://doi.org/10.1093/mnras/sty2206)

Mathews, W. G., & Prochaska, J. X. 2017, *ApJL*, 846, L24, doi: [10.3847/2041-8213/aa8861](https://doi.org/10.3847/2041-8213/aa8861)

McCarthy, I. G., Schaye, J., Ponman, T. J., et al. 2010, *Monthly Notices of the Royal Astronomical Society*, 406, 822, doi: [10.1111/j.1365-2966.2010.16750.x](https://doi.org/10.1111/j.1365-2966.2010.16750.x)

McQuinn, M. 2013, *The Astrophysical Journal*, 780, L33, doi: [10.1088/2041-8205/780/2/l33](https://doi.org/10.1088/2041-8205/780/2/l33)

Mellier, Y., Abdurro'uf, Acevedo Barroso, J. A., et al. 2025, *Astronomy & Astrophysics*, 697, A1, doi: [10.1051/0004-6361/202450810](https://doi.org/10.1051/0004-6361/202450810)

Miller, M. J., & Bregman, J. N. 2013, *ApJ*, 770, 118, doi: [10.1088/0004-637X/770/2/118](https://doi.org/10.1088/0004-637X/770/2/118)

Murphy, E. J., Condon, J. J., Schinnerer, E., et al. 2011, *The Astrophysical Journal*, 737, 67, doi: [10.1088/0004-637X/737/2/67](https://doi.org/10.1088/0004-637X/737/2/67)

Naiman, J. P., Pillepich, A., Springel, V., et al. 2018, *Monthly Notices of the Royal Astronomical Society*, 477, 1206–1224, doi: [10.1093/mnras/sty618](https://doi.org/10.1093/mnras/sty618)

Navarro, J. F., Frenk, C. S., & White, S. D. M. 1997, *ApJ*, 490, 493, doi: [10.1086/304888](https://doi.org/10.1086/304888)

Nelson, D., Pillepich, A., Springel, V., et al. 2017, *Monthly Notices of the Royal Astronomical Society*, 475, 624–647, doi: [10.1093/mnras/stx3040](https://doi.org/10.1093/mnras/stx3040)

Nelson, D., Springel, V., Pillepich, A., et al. 2021, *The IllustrisTNG Simulations: Public Data Release*, <https://arxiv.org/abs/1812.05609>

Ocker, S. K., & Cordes, J. M. 2024, *Research Notes of the AAS*, 8, 17, doi: [10.3847/2515-5172/ad1bf1](https://doi.org/10.3847/2515-5172/ad1bf1)

Ocker, S. K., Cordes, J. M., & Chatterjee, S. 2020, *The Astrophysical Journal*, 897, 124, doi: [10.3847/1538-4357/ab98f9](https://doi.org/10.3847/1538-4357/ab98f9)

Oppenheimer, B. D., Babul, A., Bahé, Y., Butsky, I. S., & McCarthy, I. G. 2021, *Universe*, 7, 209, doi: [10.3390/universe7070209](https://doi.org/10.3390/universe7070209)

Petroff, E., Hessels, J. W. T., & Lorimer, D. R. 2019, *The Astronomy and Astrophysics Review*, 27, doi: [10.1007/s00159-019-0116-6](https://doi.org/10.1007/s00159-019-0116-6)

Pillepich, A., Nelson, D., Hernquist, L., et al. 2017, *Monthly Notices of the Royal Astronomical Society*, 475, 648–675, doi: [10.1093/mnras/stx3112](https://doi.org/10.1093/mnras/stx3112)

Planck Collaboration, Aghanim, N., Akrami, Y., et al. 2020, *A&A*, 641, A6, doi: [10.1051/0004-6361/201833910](https://doi.org/10.1051/0004-6361/201833910)

Popesso, P., Biviano, A., Marini, I., et al. 2024, The hot gas mass fraction in halos. From Milky Way-like groups to massive clusters, <https://arxiv.org/abs/2411.16555>

Prochaska, J. X., & Zheng, Y. 2019, MNRAS, 485, 648, doi: [10.1093/mnras/stz261](https://doi.org/10.1093/mnras/stz261)

Ravi, V., Catha, M., Chen, G., et al. 2025, The Astronomical Journal, 169, 330, doi: [10.3847/1538-3881/adc725](https://doi.org/10.3847/1538-3881/adc725)

Reischke, R., & Hagstotz, S. 2025, A first measurement of baryonic feedback with Fast Radio Bursts, <https://arxiv.org/abs/2507.17742>

Reischke, R., Neumann, D., Bertmann, K. A., Hagstotz, S., & Hildebrandt, H. 2024, Calibrating baryonic feedback with weak lensing and fast radio bursts, <https://arxiv.org/abs/2309.09766>

Schaan, E., Ferraro, S., Amodeo, S., et al. 2021, Physical Review D, 103, doi: [10.1103/physrevd.103.063513](https://doi.org/10.1103/physrevd.103.063513)

Schawinski, K., Thomas, D., Sarzi, M., et al. 2007, Monthly Notices of the Royal Astronomical Society, 382, 1415, doi: [10.1111/j.1365-2966.2007.12487.x](https://doi.org/10.1111/j.1365-2966.2007.12487.x)

Schneider, A., Teyssier, R., Stadel, J., et al. 2019, Journal of Cosmology and Astroparticle Physics, 2019, 020–020, doi: [10.1088/1475-7516/2019/03/020](https://doi.org/10.1088/1475-7516/2019/03/020)

Semboloni, E., Hoekstra, H., Schaye, J., van Daalen, M. P., & McCarthy, I. G. 2011, Monthly Notices of the Royal Astronomical Society, 417, 2020–2035, doi: [10.1111/j.1365-2966.2011.19385.x](https://doi.org/10.1111/j.1365-2966.2011.19385.x)

Shah, V., Shin, K., Leung, C., et al. 2025, The Astrophysical Journal Letters, 979, L21, doi: [10.3847/2041-8213/ad9ddc](https://doi.org/10.3847/2041-8213/ad9ddc)

Shannon, R. M., Bannister, K. W., Bera, A., et al. 2025, Publications of the Astronomical Society of Australia, 42, doi: [10.1017/pasa.2025.8](https://doi.org/10.1017/pasa.2025.8)

Sharma, K., Krause, E., Ravi, V., et al. 2025a, Probing baryonic feedback and cosmology with 3×2-point statistic of FRBs and galaxies, <https://arxiv.org/abs/2509.05866>

Sharma, K., Krause, E., Ravi, V., et al. 2025b, The Astrophysical Journal, 989, 81, doi: [10.3847/1538-4357/adeca4](https://doi.org/10.3847/1538-4357/adeca4)

Sharma, K., Ravi, V., Connor, L., et al. 2024, Nature, 635, 61, doi: [10.1038/s41586-024-08074-9](https://doi.org/10.1038/s41586-024-08074-9)

Siegel, J., Amon, A., McCarthy, I. G., et al. 2025, Joint X-ray, kinetic Sunyaev-Zeldovich, and weak lensing measurements: toward a consensus picture of efficient gas expulsion from groups and clusters, <https://arxiv.org/abs/2509.10455>

Spergel, D., Gehrels, N., Breckinridge, J., et al. 2013, Wide-Field InfraRed Survey Telescope-Astrophysics Focused Telescope Assets WFIRST-AFTA Final Report, <https://arxiv.org/abs/1305.5422>

Springel, V., Di Matteo, T., & Hernquist, L. 2005, ApJL, 620, L79, doi: [10.1086/428772](https://doi.org/10.1086/428772)

Springel, V., Pakmor, R., Pillepich, A., et al. 2017, Monthly Notices of the Royal Astronomical Society, 475, 676–698, doi: [10.1093/mnras/stx3304](https://doi.org/10.1093/mnras/stx3304)

Sunyaev, R. A., & Zeldovich, Y. B. 1972, Comments on Astrophysics and Space Physics, 4, 173

Takahashi, R., Ioka, K., Shirasaki, M., & Osato, K. 2025, Measurement of angular cross-correlation between the cosmological dispersion measure and the thermal Sunyaev–Zeldovich effect, <https://arxiv.org/abs/2511.02155>

Tendulkar, S. P., Bassa, C. G., Cordes, J. M., et al. 2017, The Astrophysical Journal Letters, 834, L7, doi: [10.3847/2041-8213/834/2/L7](https://doi.org/10.3847/2041-8213/834/2/L7)

Tinker, J., Kravtsov, A. V., Klypin, A., et al. 2008, ApJ, 688, 709, doi: [10.1086/591439](https://doi.org/10.1086/591439)

Tumlinson, J., Peeples, M. S., & Werk, J. K. 2017, Annual Review of Astronomy and Astrophysics, 55, 389–432, doi: [10.1146/annurev-astro-091916-055240](https://doi.org/10.1146/annurev-astro-091916-055240)

Turk, M. J., Smith, B. D., Oishi, J. S., et al. 2011, ApJS, 192, 9, doi: [10.1088/0067-0049/192/1/9](https://doi.org/10.1088/0067-0049/192/1/9)

Vedantham, H. K., & Phinney, E. S. 2019, MNRAS, 483, 971, doi: [10.1093/mnras/sty2948](https://doi.org/10.1093/mnras/sty2948)

Voit, G. M. 2019, ApJ, 880, 139, doi: [10.3847/1538-4357/ab2bfd](https://doi.org/10.3847/1538-4357/ab2bfd)

Wang, H., Masui, K., Andrew, S., et al. 2025, Measurement of the DispersionxGalaxy Cross-Power Spectrum with the Second CHIME/FRB Catalog, <https://arxiv.org/abs/2506.08932>

Werk, J. K., Prochaska, J. X., Tumlinson, J., et al. 2014, The Astrophysical Journal, 792, 8, doi: [10.1088/0004-637x/792/1/8](https://doi.org/10.1088/0004-637x/792/1/8)

Wu, X., & McQuinn, M. 2023, The Astrophysical Journal, 945, 87, doi: [10.3847/1538-4357/acbc7d](https://doi.org/10.3847/1538-4357/acbc7d)

Yamasaki, S., & Totani, T. 2020, The Astrophysical Journal, 888, 105, doi: [10.3847/1538-4357/ab58c4](https://doi.org/10.3847/1538-4357/ab58c4)

Yang, X., Xu, H., He, M., et al. 2021, The Astrophysical Journal, 909, 143, doi: [10.3847/1538-4357/abddb2](https://doi.org/10.3847/1538-4357/abddb2)

Yao, J. M., Manchester, R. N., & Wang, N. 2017, The Astrophysical Journal, 835, 29, doi: [10.3847/1538-4357/835/1/29](https://doi.org/10.3847/1538-4357/835/1/29)

Zhang, Y., Comparat, J., Ponti, G., et al. 2024, Astronomy & Astrophysics, 690, A267, doi: [10.1051/0004-6361/202449412](https://doi.org/10.1051/0004-6361/202449412)